

# A Method of Structural Load Prediction for High-Speed Planing Craft

Richard H. Akers, P.E. (SNAME M)

Maine Marine Composites LLC, Portland, Maine, USA

The lack of information about hydrodynamic loads is an obstacle in the structural design of high-speed planing boats. A method is proposed to derive panel pressures from a time-domain motion simulator. The simulator predicts planing boat motion by calculating forces using first principles and semi-empirical algorithms, combining the forces, and integrating the results to solve the equations of motion. Integral to the time-domain simulator algorithm is a calculation of longitudinal pressures at every timestep. The sectional pressures are expanded into transverse pressure distributions using models from Smiley (1951) for transverse pressure distributions in the forward, chines-dry region and the aft, chines-wet region. A load-mapping software tool transfers pressure distributions to a finite element analysis program. Three validation efforts were performed by comparing simulated and measured quasi-static hull pressures published for a prismatic planing hull and a 20.5 foot fiberglass ski boat operating at constant speeds, and dynamic pressures on the hull of a recreational aluminum fishing boat operating in waves.

## INTRODUCTION

The objective of this project is to develop and verify a practical method to use time domain simulation to drive structural design of high speed planing craft. Existing and developmental time-domain simulators will be enhanced and modified so as to calculate panel pressures, vessel kinematics, and loads for use in Finite Element Method (FEM) programs for structural analysis. Specifically, low aspect ratio strip theory will be extended to predict transient slamming loads created when a high-speed craft travels through irregular seas. The new analysis method must meet the following requirements:

- Predict transient hydrodynamic panel pressures for use in Finite Element Method programs.
- Predict velocities, rates and accelerations for use in FEM programs.
- Calculate instantaneous shear forces and longitudinal bending moments for comparison and verification of results.

Maine Marine Composites (MMC) has been working continuously for almost two decades on a computer program to predict the surge, heave and pitch motion of a planing boat in regular and irregular seas. The simulator was developed from algorithms described in a computer program developed and published by Ernest Zarnick (1978) of David W. Taylor Naval Ship R & D Center. Instantaneous motions of a planing boat are predicted by:

- Calculating the forces on each one of hundreds of hydrodynamic stations (sections) by using the following algorithms: impacting wedge, linear 2D buttock flow, viscous drag using Reynold's Number-based drag coefficients, and crossflow drag in fully-wetted regions
- Adding the sectional force components together in a weighted sum using weighting coefficients derived from more than 100 model and full-scale tests
- Calculating the added mass for each section using empirical formulas based on the sectional deadrise
- Integrating the forces and added masses for each degree of freedom
- Multiplying the inverted mass matrix times the force vector to obtain the accelerations in surge, heave and pitch; and then integrating the accelerations to find velocities and rates, and then integrating again to find positions and angles.

In the Ship Structures Committee (SSC) Project SR-1470 the time-domain simulator program was modeled to export point pressures within an operator-specified subset of the entire geometric mesh describing the hull. With some interpolation to match the pressures obtained from the simulator with the mesh used in the FEM analysis, the strain in the structural panels of the planing boat can be predicted. This strain can be used to test the capability of the boat hull to withstand a particular sea state without damage.

The specific goal of this SSC project was to show that sectional pressures calculated by the simulator can be converted to panel pressures which can be used in a Finite Analysis Method (FEM) program to predict stress and strain in the hull structure.

## Background

There is on-going interest in high-speed planing boats, especially for government patrol boats. The USCG is in the middle of a long-term acquisition program for the RB-S and RB-M patrol craft. USSOCOM has issued a contract for the CCM Mark I, a replacement craft for the workhorse 11m RIB. In the civilian sector, high-speed craft are important for new, competitive ferry services and possibly for high-speed freight services, both regulated by US Coast Guard.

Structural assessment of these craft has an important impact on their operational safety. A major problem in the design of high-speed planing boats such as fast ferries and patrol craft is predicting the panel loads for structural analysis. It is very difficult to predict the loads for quasi-static operation of planing boats, and even more difficult to predict the instantaneous loads in irregular sea states. Often techniques such as computational fluid dynamics (CFD) are used to predict hydrodynamic loads, but these methods are computationally intensive and cannot be used in long time-domain simulations of planing craft.

To illustrate the difficulty of designing high-speed planing craft, the Mk V is an 82-foot boat used by the Special Operations Forces with an estimated top speed of 47-50+ knots in SS2, and a cruising speed of 25-35 knots in SS3. A requirement for the Mk V was that it be designed to meet the 1990 ABS *Guide for Building and Classing High Speed Craft* (Codega, 2014). The vessel's severe missions resulted in structural failures and injuries to crew and passengers. Since that time ABS Guide has evolved into the present-day version, *Rules for Building and Classing High Speed Naval Craft* (ABS, 2014). Part 3, Chapter 2, Section 2, "Design Pressures," of this standard addresses

bottom loading to be used for structural design. The primary method of estimating pressures is to use formulas for bottom slamming and hydrostatic pressure. These formulas have been derived from a combination of first principle and empirical methods, and are hull-location specific. Alternatively, the ABS Rules (3-1-3, Section 9.1) state that hydrodynamic "... analysis software formulations derived from linear idealizations [panel methods and strip theory] are sufficient. Enhanced bases of analysis may be required so that non-linear loads, such as hull slamming, may be required. The adequacy of the selected software is to be demonstrated to the satisfaction of ABS." These methods are efficient and appropriate for the design of conventional boats to be used in well understood missions, but may fall short for the design of new hullforms or structures designed for new, demanding missions. A more accurate method of predicting instantaneous, local structural loads is required for the design of future high-speed patrol boats and high-speed ferries.

Empirical algorithms have a limited range of applicability and are not well suited to time domain simulation. Spencer (1975) proposed a methodology for structural design of aluminum crewboats using Savitsky's method (1964) to predict the trim angle of the vessel, data from Fridsma (1971) to predict peak accelerations, and a technique from Heller and Jasper (1960) to predict hull pressure distributions. Given a pressure distribution, engineers can calculate maximum frame spacings and minimum panel thicknesses. This method is an historical basis for the dynamic pressure used in the USCG's NVIC 11-80 (1980). Unfortunately the method makes assumptions about sea states, missions, and hull geometry. Any significant deviations from these assumptions introduce uncertainty into the design process. In 2005 SSC funded a project to study and compare "...the application, requirements and methods for the structural design of high speed craft..." used by various classification societies (Stone, 2005). Classification society rules use empirical formulas to predict vertical accelerations, which are used in structural design calculations. A more direct method would be to use time-domain simulation to predict panel pressures for structural design.

According to Akers (1999a, 1999b) and Rosén (2004) planing hull simulation programs based on low aspect ratio strip theory have been in existence for several decades. These programs can predict the vertical accelerations of a planing monohull operating in a seaway with good engineering accuracy.

### Justification for Project

The *ABS Rules for Building and Classing High Speed Naval Craft* (ABS, 2014) recognizes that time domain simulation is an effective way of predicting hull pressures for structural analysis of high speed craft. Section 3-1-3 of the *Guide* says:

"3.5.7(a) Global Slamming Effects. The simplified formulae ... may be used to account for global slamming effects in the preliminary design stage. For detailed analysis, a direct time-domain simulation involving short-term predictions are to be used for the global strength assessment of monohulls. In most cases

involving high speeds, the absolute motions or relative motions will be of such large amplitude that nonlinear calculations will be required...

"3.5.7(b) Local Impact Loads. Panel structures with horizontal flat or nearly flat surfaces such as a wet deck of a multi-hull craft will need to be hydroelastically modeled, where in the dynamics of the fluid and the elastic response of the plate and stiffeners are simultaneously modeled."

### SIMULATION OF PLANING HULLS

The time-domain simulator used as the basis for this project calculates sectional forces, integrates the forces longitudinally, and solves for the boat accelerations. The primary goal of this project is to expand the sectional forces into panel pressures which can be used in structural analyses. At each time step the time-domain simulator calculates sectional pressure contributions from the following sources:

- Impacting wedge (low aspect ratio strip theory).
- Low aspect ratios 2D ideal flow to model buttock flow
- Crossflow drag for sections in the chines-wet region
- Viscous drag based on the mean wetted length
- Hydrostatic buoyancy

The results are weighted and added together on a section-by-section basis to calculate an array sectional force vectors.

At each time step, the simulator:

1. Calculates the force vector and moment vector contributed by each station (refer to Appendix 1).
2. Calculates the added mass contributed by each station
3. Integrates the station force and moment vectors to find the total force vector and moment vector
4. Integrates the added mass over the entire hull to find the total added mass and added pitch inertia
5. Solves the equations of motion to find instantaneous angular and radial accelerations:
 
$$|A| = (|M| + |\text{Added M}|)^{-1} * |\text{Total Force/Moment}|$$
6. Integrates the accelerations to find velocities and the velocities/angular rates to find positions/angles

The sectional force and moment vectors calculated in Step 1 are the basis for calculating the vector forces exported to FEA.

### CALCULATING PRESSURES FOR STRUCTURAL ANALYSIS

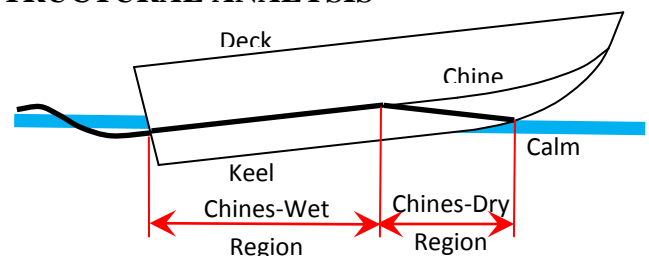


Figure 1 Planing Regions

The transverse pressure distributions can be categorized by their region of operation (refer to Figure 1). Starting at the bow of the

planing boat, the most forward wetted point on the keel occurs at the calm waterline. Moving aftward, the water rises above the calm waterline because the water displaced by the boat piles up to port/starboard, resulting in an increase of the sectional draft. Eventually the piled-up water reaches the chine. The “chines-dry region” is the range between the most forward wetted point and the station for which the pile-up water reaches the chine. The transverse flow separates off of the chine, so the piled-up water stops at the chine. The distance abaft the end of the “chines-dry region” is, of course, called “chines-wet.”

From many model tests (e.g. Kapryan, 1955; Broglia, et. al. 2010) it is apparent that the transverse pressure distribution follows a curve that resembles the curves in Figure 2. The similarity between the pressure distributions at different longitudinal locations is apparent in this figure. The distributions with a peak occur in the “chines-dry” region, while the ones without a peak occur in the “chines-wet” region.

### Transverse Pressure Distribution

As seen in Figure 2 the transverse pressure distribution in the chines-dry region is dramatically different than that in the chines-wet region. In the chines-dry region the pressure reaches a peak value along a stagnation line and drops off quickly toward the keel. After the stagnation line reaches the chine in the chines-wet region, the pressure distribution becomes much more constant, tapering off as it nears the chine.

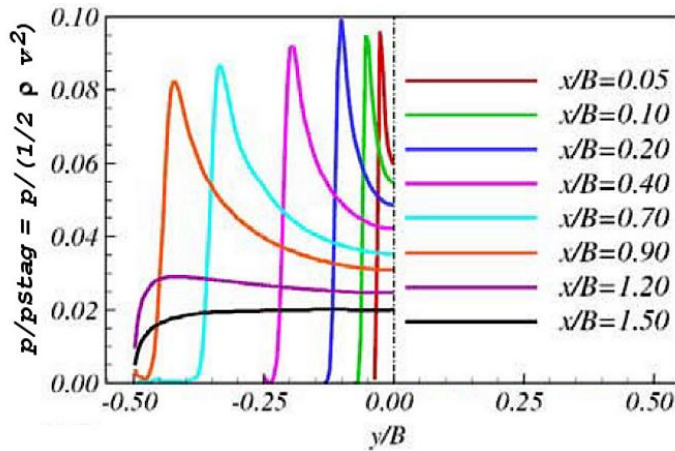


Figure 2 Transverse pressure distribution measured on boat with 0-heel angle. “y/B=0.05” is bow and “y/B=1.50” is stern (Broglia, et. al., 2010, Figure 7). Curves with peaks are in chines-dry region, curves at x/B=1.2 and 1.5 are in chines-wet region.

The procedure for calculating pressure loads at any point on the hull is to calculate the total sectional pressure (force/unit length) and use the models summarized in Smiley (1951) to calculate a transverse pressure distribution from the sectional forces. Smiley suggests two different methods of modeling the pressure distribution, one for the forward chines-dry region and one for the aft chines-wet region of the boat.

### Modeling the Transverse Pressure Distribution: Chines-Dry Region

The transverse pressure distribution in the chines-dry region is modeled using Equations 1, 2 and 3. The variable K is the water-rise ratio.

$$K \approx \frac{\pi}{2} \left( 1 - \frac{3 \tan^2 \beta \cos \beta}{1.7 \pi^2} - \frac{\tan \beta \sin^2 \beta}{3.3 \pi} \right) \quad (1)$$

The deadrise  $\beta$  is assumed to be constant for each station, defined as the angle between the keel point and the chine point. For computational efficiency a spline curve is precalculated to compute K from  $\beta$  (refer to Figure 4).

Pierson (1948) and Pierson and Leshover (1950) suggest Equation 2 to calculate a modified deadrise  $\theta$  taking into account the running trim of the boat. The value K was precalculated using the spline curve described above.

$$\tan(\theta) = \frac{\pi}{2} \sqrt{\frac{\sin^2 \beta + K^2 \tan^2 \tau}{K^2 - 2K \sin^2 \beta - K^2 \sin^2 \beta \tan^2 \tau}} \quad (2)$$

Smiley’s transverse pressure distribution uses this in the form of  $\cot(\theta) = 1/\tan(\theta)$ . The transverse pressure distribution is modeled by Equation 3 with an appropriate scale factor.

$$\frac{p(\hat{\eta})}{p_{SECTION}} \propto \left[ \frac{\pi \cot(\theta)}{\sqrt{1 - (\hat{\eta}/c)^2}} - \frac{1}{(\hat{\eta}/c)^2 - 1} \right] \quad (3)$$

Equation 3 includes a variable  $\eta$  which is related to the transverse distance from the keel toward the chine. The term  $(\eta/c)$  represents the normalized wetted half beam ranging from 0 to 1. The equation goes to  $-\infty$  when  $\eta=c$ , corresponding to the pressure at the outer edge of the wetted surface c. The pressure curve passes through 0 close to that point, and the zero crossing is the effective outer edge of the wetted beam model. In other words the model is not accurate over the entire range of normalized half beam, but has to be scaled slightly. A value  $\hat{\eta}$  is defined that maps  $\eta$  from the keel to the zero crossing. At each time-step, the trim angle  $\tau$  is known, so a second constant c1 is calculated.

$$c1 = 2 \sqrt{\frac{K(K(1 - \sin^2 \beta \tan^2 \tau) - 2 \sin^2 \beta)}{\sin^2 \beta + K^2 \tan^2 \tau}} \quad (4)$$

Instead of ranging from 0 to 1, the value of  $\hat{\eta}$  ranges from 0 to  $\hat{\eta}_{MAX}$  as calculated as in Equation 5.

$$\hat{\eta}_{MAX} = \frac{1}{2} \sqrt{2 c1 \sqrt{c1^2 + 4} - 2 c1^2} \quad (5)$$

A factor of proportionality is chosen so that the integral of Equation 3 from  $\hat{\eta} = 0$  to  $\hat{\eta}_{MAX}$  is equal to 1. The direct integral of this formula can be shown to be Equation 6. The total transverse pressure calculated by this formula over the entire wetted beam is equal to the sectional pressure.

$$\hat{p}_{TOTAL} = c1 \text{asin}(\hat{\eta}_{MAX}) + \hat{\eta}_{MAX} + \frac{1}{2} \ln \left( \frac{1 - \hat{\eta}_{MAX}}{1 + \hat{\eta}_{MAX}} \right) \quad (6)$$

The scale factor required to make Equation 3 an equality is  $\hat{p}_{TOTAL}$ . Figure 3 is a chart of the transverse pressure for three different values of deadrise  $\beta$ , all shown for a constant trim  $\tau = 4$  degrees.

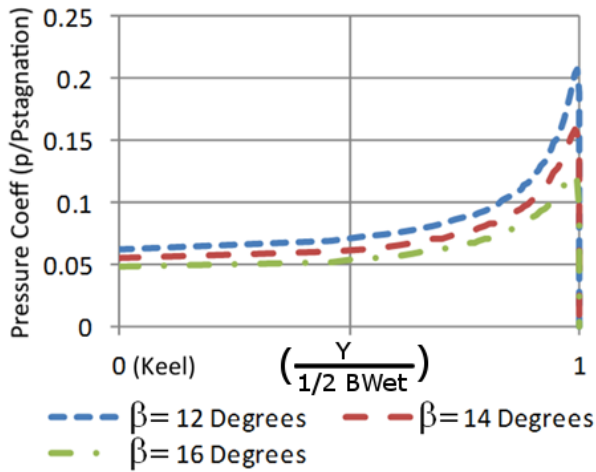


Figure 3 Sample chines-dry transverse pressure distributions for three different deadrise angles. All three distributions were calculated at a running trim of 4 degrees.

**Modeling the Transverse Pressure Distribution: Chines-Wet Region**

The transverse pressure distribution in the Chines-Wet Region does not have the bump at the stagnation line that the Chines-Dry distribution has. Instead it starts with a flat region near the keel and rolls off as it approaches the chine (refer to Figure 2, curve “y/B=1.5”). Smiley (1951) uses the results of a derivation from Korvin-Kroukovsky and Chabrow (1948) to model the pressure distribution in the chines-wet region. Variables in the following equations are:

b	Half beam of boat	h	(Constant)
$\beta$	Deadrise, radians	k	(Constant)
e	Auxiliary variable, radians	$\eta$	Transverse distance from keel, positive toward chine

Equation 7 and Equation 8 map the deadrise  $\beta$  to a constant value k. For efficiency an array of pairs of ( $\beta$ , k) are precalculated and mapped with a spline function so that k can be calculated quickly for any value of  $\beta$  (refer to Figure 4).

$$h = \frac{\pi - 2\beta}{\pi} \quad (7)$$

$$\frac{1}{k} = 4 \cos\beta \int_0^{2\pi} (1 + \sin(\epsilon))^h (\cos(\epsilon))^{1-h} \sin(\epsilon) d\epsilon \quad (8)$$

Equation 9 maps the transverse location  $\eta$  to a non-dimensional value  $\epsilon$  and Equation 10 maps  $\epsilon$  to non-dimensionalized pressure:

$$\frac{\eta}{b} = 2k \cos\beta \int_{\epsilon}^{2\pi} (1 + \sin(\epsilon))^h (\cos(\epsilon))^{1-h} \sin(\epsilon) d\epsilon \quad (9)$$

$$\frac{p(\eta)}{P_{Section}} \propto 1 - \left( \frac{\cos(\epsilon)}{1 + \sin(\epsilon)} \right)^{2h} \quad (10)$$

**Distributing the Force and Moment between Panels**

At each time step the simulator calculates a 3-component longitudinal force vector contributed by each station. These

force vectors are not normal to the hull. To calculate a pressure distribution for a point on the hull, the force vector is scaled:

- By the area of each panel =  $\Delta x * \Delta y$ , and
- By the vertical component of the panel normal so that the integral of the vertical components of pressure add up to the required longitudinal section pressure.

It is assumed that the panel normal to the panel is primarily in the Y-Z plane and that there is little longitudinal variation in panels.

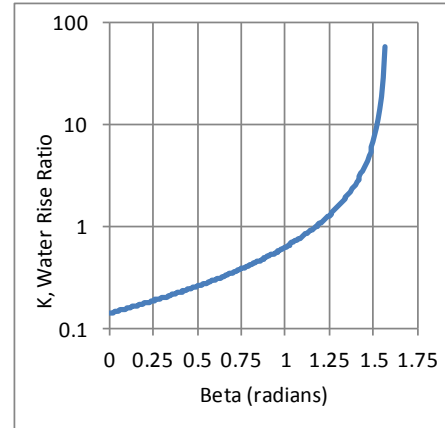


Figure 4 Constant used in chines-wet transverse pressure calculations, plotted versus deadrise  $\beta$

The simulation mesh and the FEA simulation will not be identical and a load mapping step is required. It is likely that some of the individual FEA panels will map to multiple simulation pressure panels and vice versa. To avoid many of these problems, a large number of pressure panels are exported for each section of the simulation model. In both the chines-dry and chines-wet regions, much of the curvature in the pressure distribution occurs near the outer edge of the wetted surface. To make sure that the pressure points exported by the simulator have sufficient density to model the rapid pressure changes, the simulator models each section with 50 pressure panels whose panel width is inversely proportional to the cube of the fraction of the distance from the keel to the chine.

**Communication between Simulator and FEA**

There are two possible approaches to using loads calculated by the time-domain simulator in an FEA tool. The simulator can export pressure values (scalars) at regular intervals or it can export force vectors at these same intervals. In most cases the force or pressure locations analyzed by the simulator do not correspond directly to locations in the FEA mesh, so an interpolation step is required. Most commercial FEA tools include support for load mapping (interpolation), while many of the open source tools do not.

**Geometry Algorithms to Export Pressures to FEA**

To export a pressure map for use in FEA:

- The FEA system creates a mesh.
- The simulator creates a scalar point cloud of pressures.

- An interpolation tool reads the FEA mesh, reads the simulation scalar data, and interpolates to find the pressure at the center of each FEA face.
- The interpolation tool exports a pressure file for the finite element analyzer.

The interpolation program was designed to take advantage of the regular section spacing in the time-domain simulator model. Sections (stations) are defined as having constant X coordinates, so the first step in the interpolations is to identify the pair of stations that bound the FEA vertex. Once the stations have been identified, the Y-coordinate of the FEA vertex is used to find the pair of offset locations in each station that bound the vertex. Finally linear interpolation between the four offset locations (two on each section) is used to calculate the pressure that corresponds to the FEA vertex. If a higher order interpolation algorithm such as quadratic interpolation was used, the time-domain simulator could export fewer pressure points, and the FEA pressure mesh might be slightly more accurate.

Special attention must be paid to the case in which there is a large FEA face covering many of simulator vertices, some with high pressure (e.g., the stagnation line in the chines-dry region) and most with low pressure or zero pressure (e.g. above the wetted surface). Interpolation is challenging because the average of all of these pressures is not necessarily the best value to use, and a polynomial interpolation may fail due to oscillations in the polynomial. In this project these problems have been addressed by using a fine mesh in both the time-domain simulator and the FEA models.

**Case Study: Aluminum Fishing Boat**

As a case study, the offsets were taken from an existing aluminum fishing boat built by Grumman (see Figure 5 and Figure 6).



Figure 5 Grumman aluminum fishing boat

The hull has formed transverse stiffeners, visible in Figure 6, that serve to limit the panel size in the hull. In addition to the transverse stiffeners, there are longitudinal strakes (not shown) in the forward sections. For purposes of this exercise, a section of panel was chosen that spans the distance uninterrupted from the keel to the formed chine.

A full 3D CAD model of the aluminum hull was created using the MultiSurf program (see Figure 7). In this figure surfaces are rendered as semi-transparent so that the complete inner structure

of the boat is visible. The goal of this study is to explore the stress imposed in this panel by the boat travelling over regular waves with a wavelength of about five boat lengths. From experience, that sea condition will cause the boat to exhibit large vertical motions, possibly launching and slamming depending on the size of the engine.



Figure 6 Structure of aluminum fishing boat. Transverse stiffeners are visible on the hull.

For this case study, a single panel was selected from the hull bottom for analysis. This panel is circled in Figure 7.

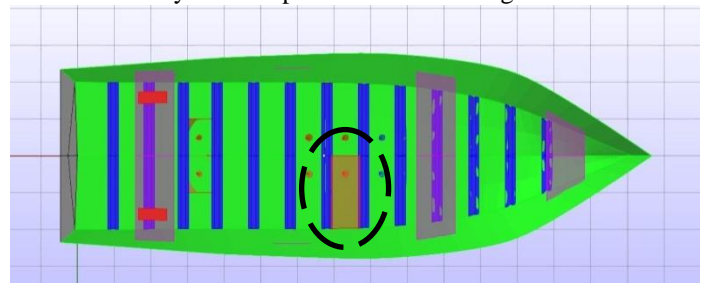


Figure 7 MultiSurf (3D CAD) model of Grumman aluminum fishing boat (third seat not shown). Test panel between aluminum transverse stiffeners is circled.

The exact dimensions of the test panel are given in Figure 8. As the test boat was on-loan from another organization it was not possible to cut into the hull to measure the hull plating thickness, nor was there historical documentation listing the hull plating thickness. For purposes of this analysis the plating was estimated to be 5.0 mm. The mechanical properties of the hull plating were assumed to be:

Young's Modulus	69 GPa (Aluminum)
Poisson ratio	0.333

The mesh created for that panel was created using a commercial meshing program, but is a regular matrix of 189 'S4' shell elements that could have been created by hand. The mesh is shown in Figure 9. The panel was modeled as being locked in

all degrees of freedom on edge nodes, considered to be consistent with the structure in the hull.

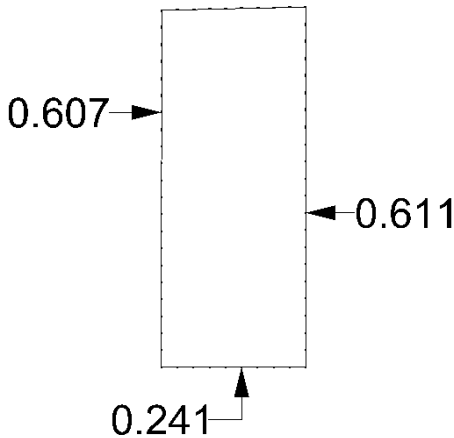


Figure 8 Test panel dimensions. The panel is not rectangular.

**Simulation Results**

The aluminum fishing boat was simulated at a constant speed of 14 knots operating in regular waves with a height (double amplitude) of 1.0 feet and a wavelength of 100 feet, about five boat lengths. The simulator predicted that the boat would perform as shown in Figure 10 and that the vertical accelerations at the center of gravity and the forward seat would be as shown in Figure 11. From the acceleration chart the boat never entirely launches out of the water because there is no protracted period with a constant -1 G acceleration. On the other hand, the boat does get subjected to some extreme loads as it

itches and heaves out of phase with the waves that it is encountering.

A set of hull pressures were calculated by the simulator at 0.1 second time steps starting at Time=7.0 seconds to Time=8.0 seconds. The hull pressures obtained from simulation using the method presented in this paper are shown Figure 12 through Figure 22.

Each hull pressure distribution was exported from the simulation program into a text file containing coordinate/pressure pairs. A load mapping program was used to interpolate between simulator vertices and FEA vertices. Finally the load mapping program was used to allocate pressure loads to the S4 quad elements in the CalculiX model. The CalculiX FEA program (Wittig, 2013) was used to estimate the Von Mises stress in the aluminum hull panel and the results are included here as Figure 23 through Figure 31. In these figures the bow is on the left side of the panel and the stern on the right. At time 0.74 seconds the panel is barely wet, so the strain indicated by the FEA program is uniformly 0 except for a small point near the keel (see Figure 27). The panel is completely dry at time steps 7.5 and 7.6, so only one strain figure is included for this case (Figure 28).

The strain pattern shows relatively low, even strain when the boat is between waves. As the boat crosses a wave the wetted surface narrows and the pressure is concentrated near the keel, finally disappearing when the panel is dry. When the panel becomes wet at the next wave the high pressure from the chines-dry region of operation appears near the keel and then spreads out to cover the entire panel.

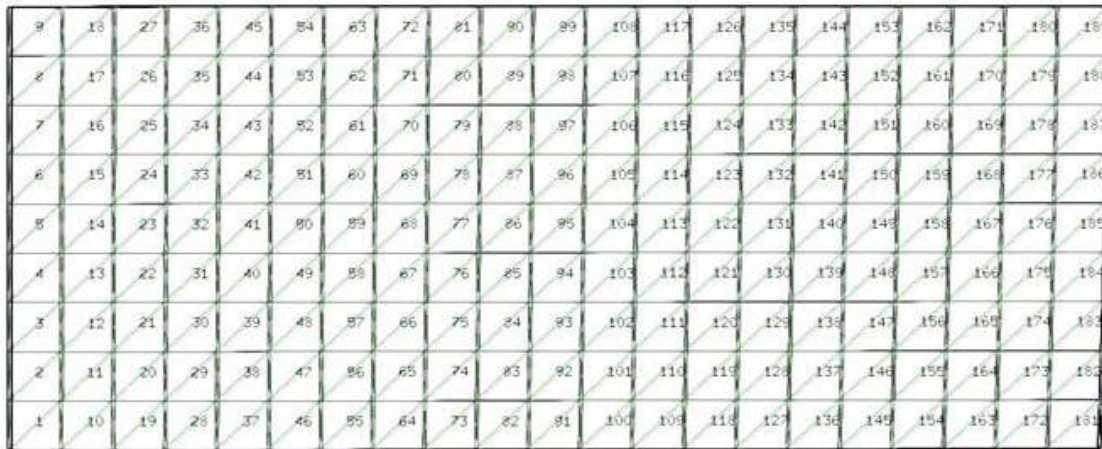


Figure 9 Mesh of fishing boat hull panel created using commercial meshing program.

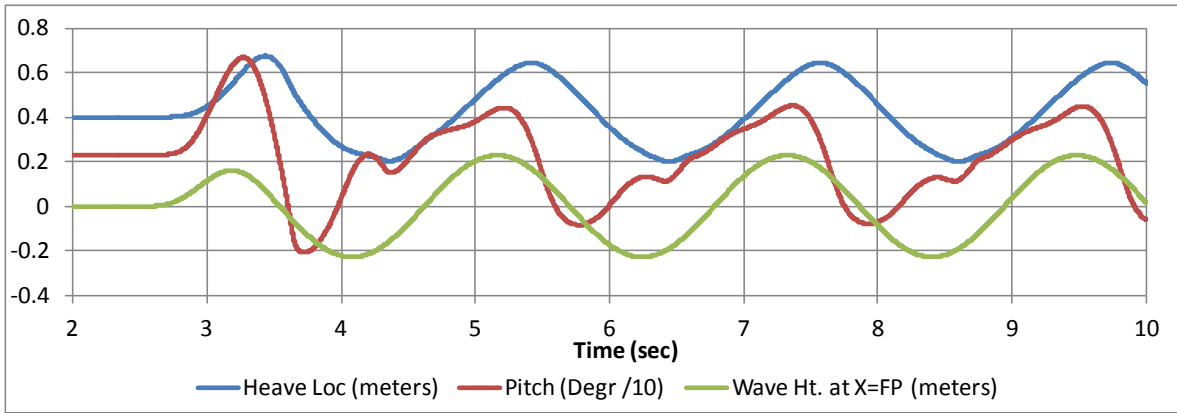


Figure 10 Motion of aluminum fishing boat in regular waves (height=1.0 feet, wavelength=100 feet) predicted by simulation.

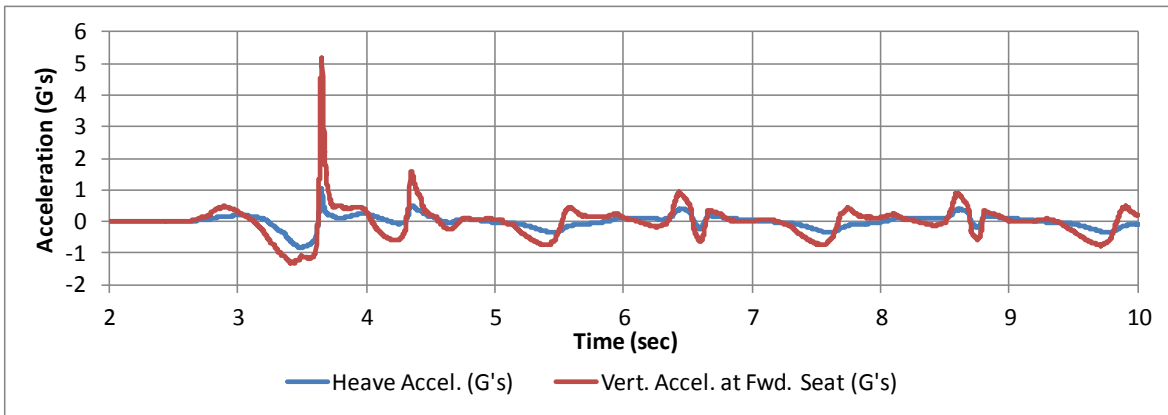


Figure 11 Accelerations on aluminum fishing boat predicted by simulation. Time series between 7 and 8 seconds were used for FEA.

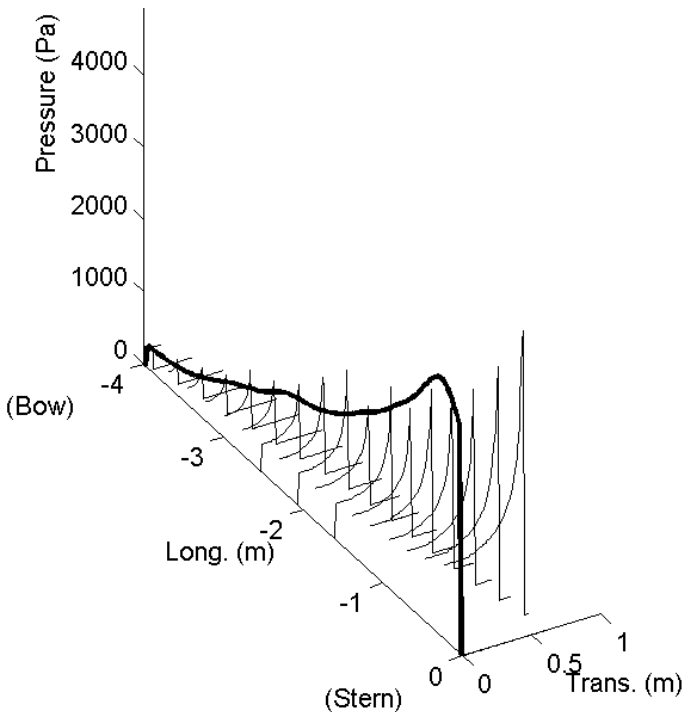


Figure 12 Trans. pressure distribution from sim., Time =7.0 sec

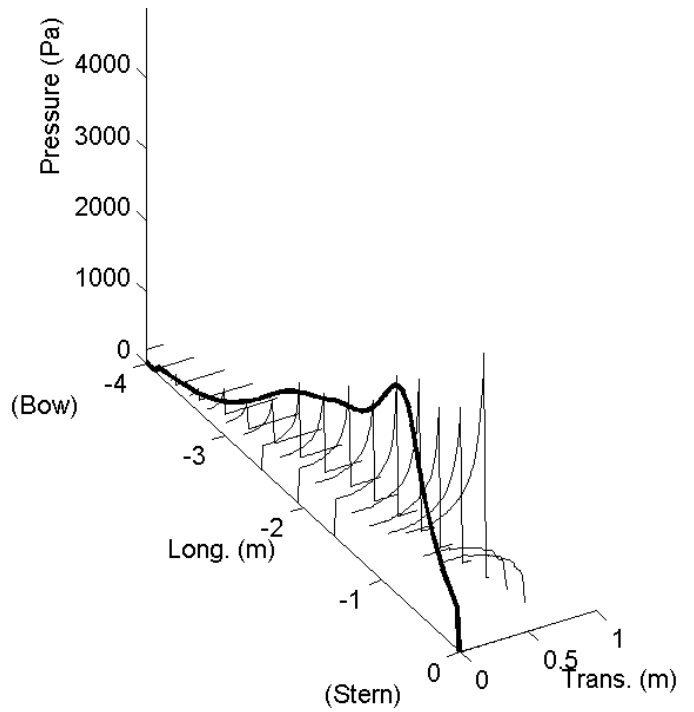


Figure 13 Trans. pressure distribution from sim., Time =7.1 sec

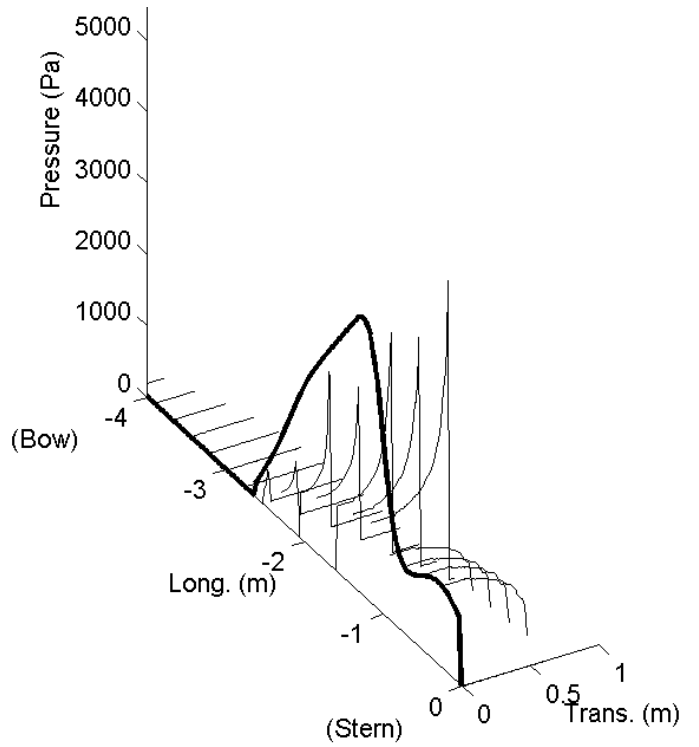
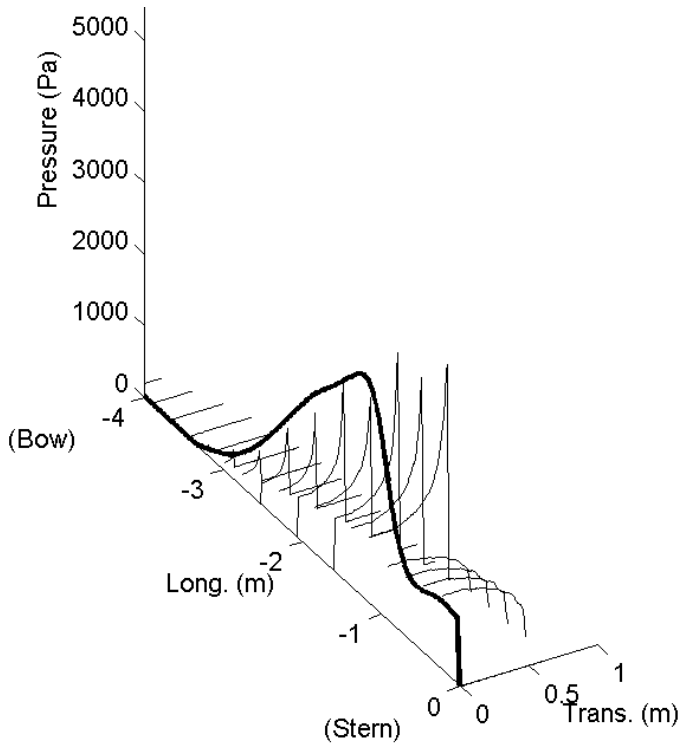


Figure 14 Trans. pressure distribution from simulation, Time =7.2 seconds

Figure 15 Trans. pressure distribution from simulation, Time =7.3 seconds

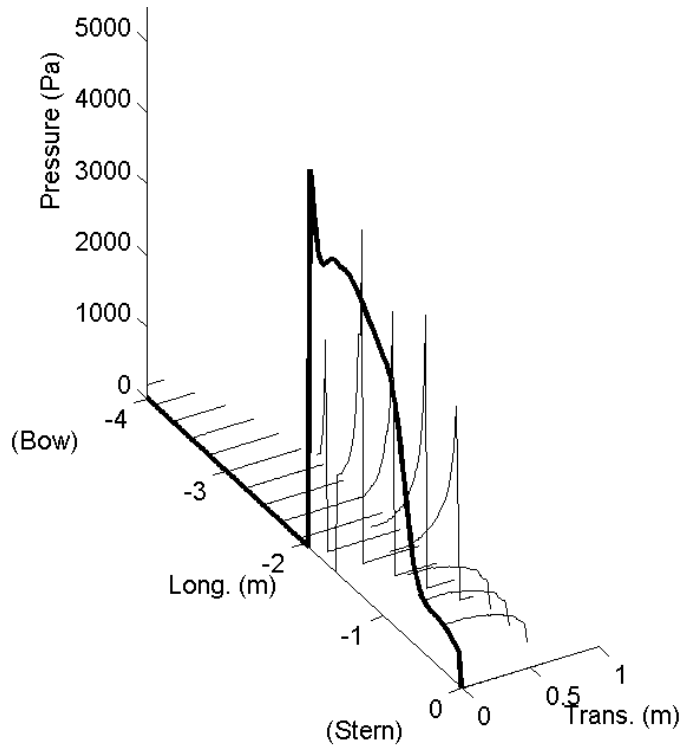
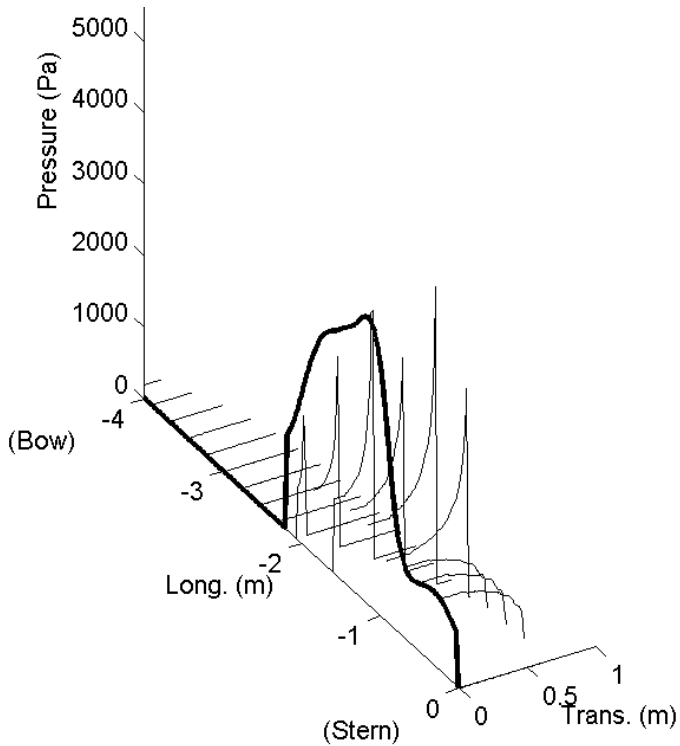


Figure 16 Trans. pressure distribution from simulation, Time =7.4 seconds

Figure 17 Trans. pressure distribution from simulation, Time =7.5 seconds

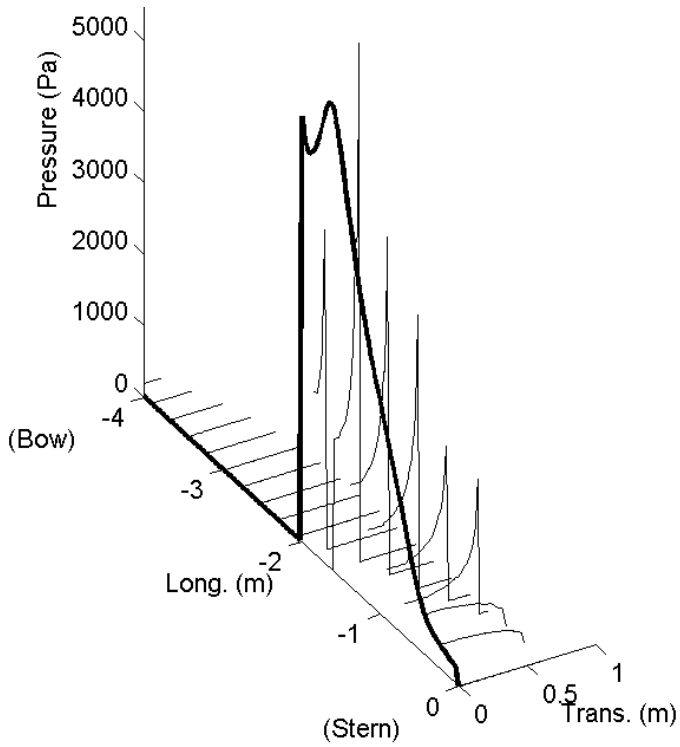


Figure 18 Trans. pressure distribution from simulation, Time =7.6 seconds

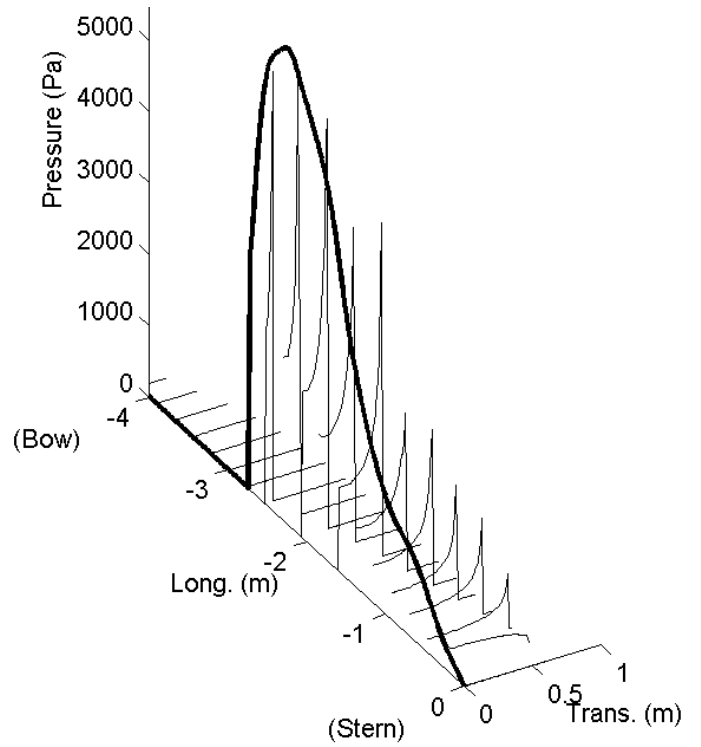


Figure 19 Trans. pressure distribution from simulation, Time =7.7 seconds

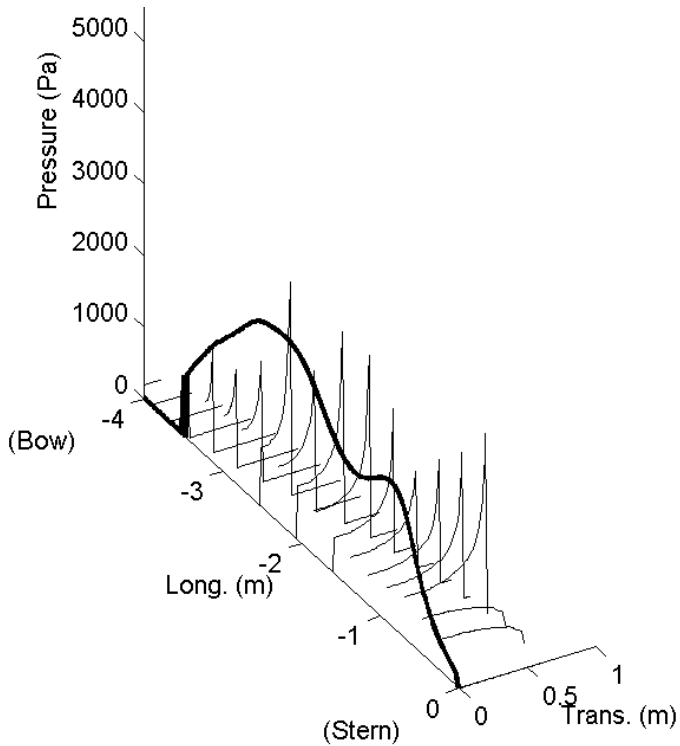


Figure 20 Trans. pressure distribution from simulation, Time =7.8 seconds

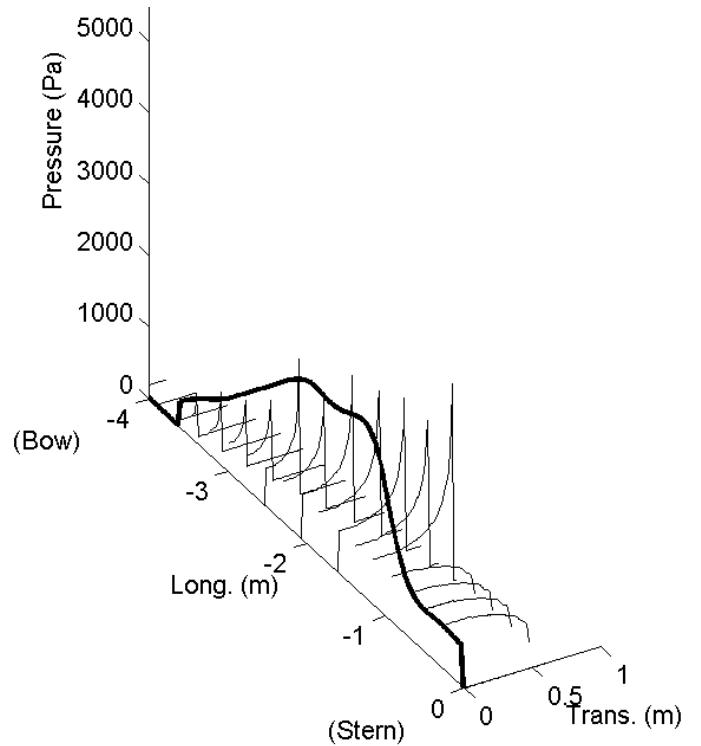


Figure 21 Trans. pressure distribution from simulation, Time =7.9 seconds

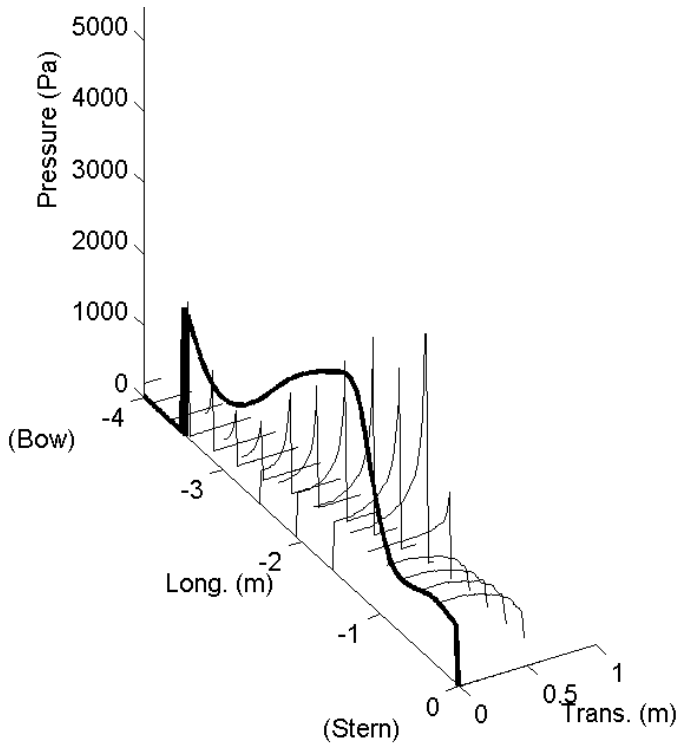


Figure 22 Trans. pressure distribution from simulation, Time =8.0 seconds

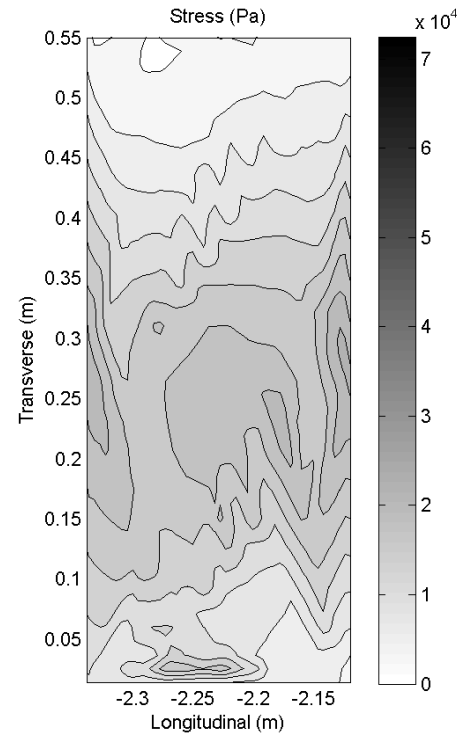


Figure 23 Stress in panel, Time=7.0

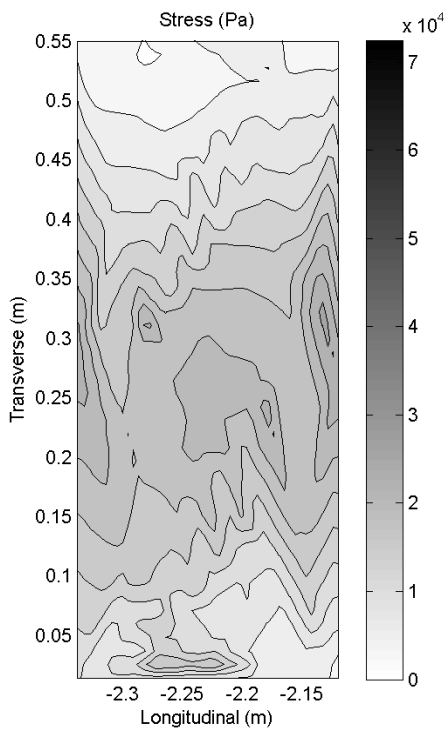


Figure 24 Stress in panel, Time=7.1

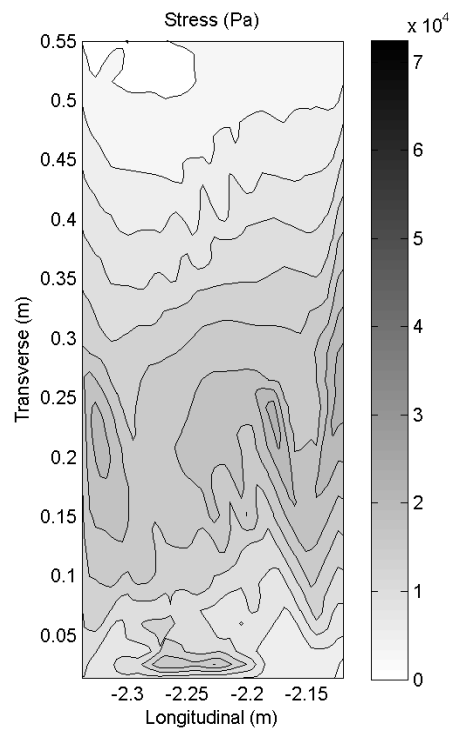


Figure 25 Stress in panel, Time=7.2

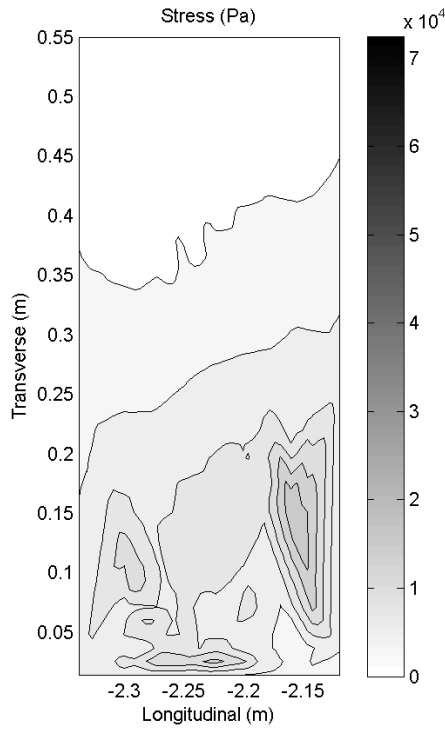


Figure 26 Stress in panel, Time=7.3

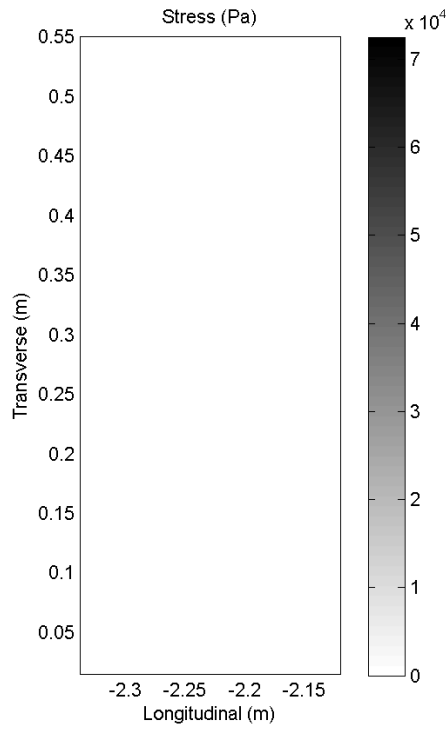


Figure 27 Stress in panel, Time=7.4-7.6

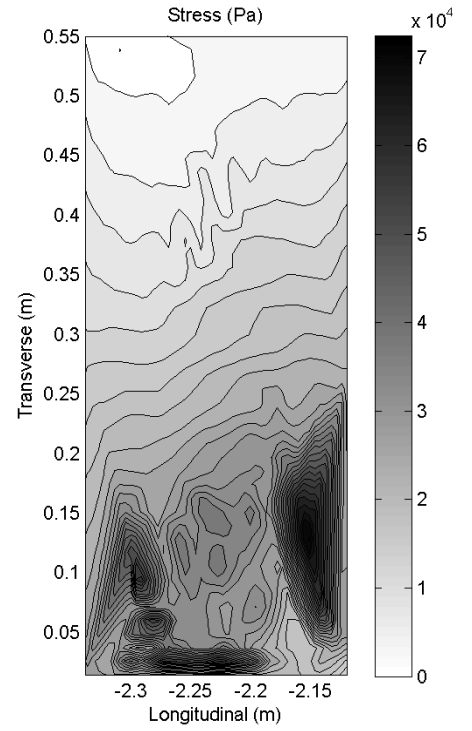


Figure 28 Stress in panel, Time=7.7

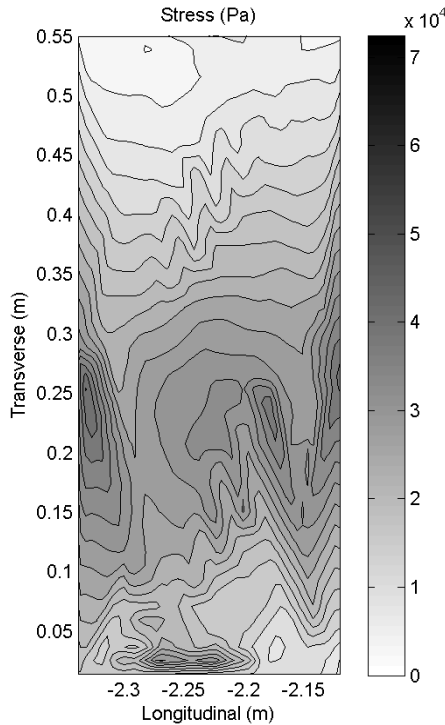


Figure 29 Stress in panel, Time=7.8

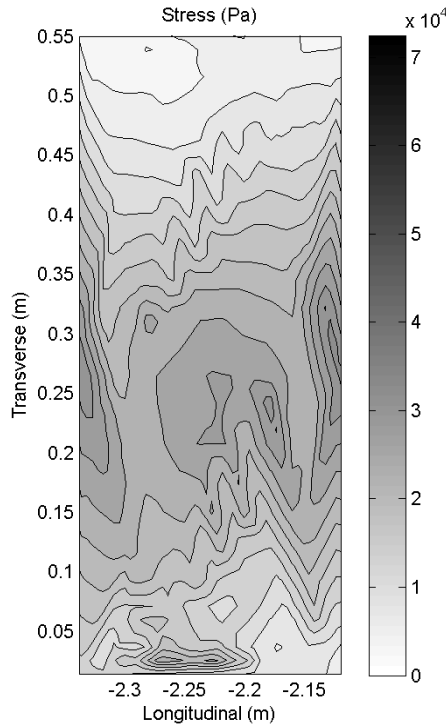


Figure 30 Stress in panel, Time=7.9

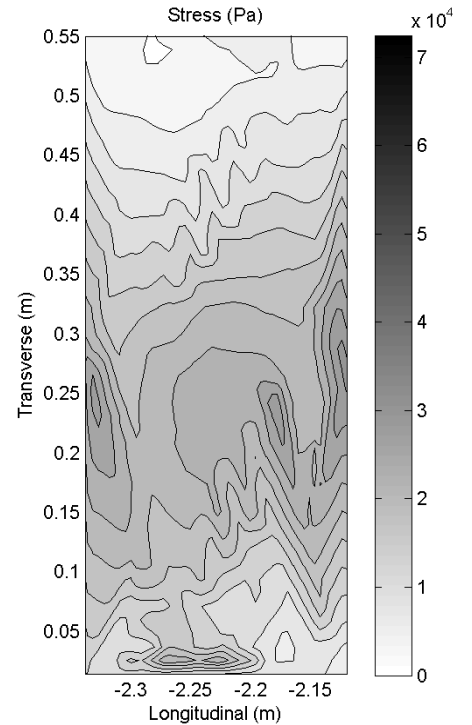


Figure 31 Stress in panel, Time=8.0

## VALIDATION

### Test Case: Recreational Planing Boat

To test the ability of the modified version of the simulator to export accurate pressures, simulated results were compared with pressure measurements taken on a ski boat built by Hydrodyne Boat Company, in Fort Wayne, Indiana. The following description of the boat is quoted from Royce (2001).

“[Hydrodyne Boat Company of Fort Wayne, IN] agreed to build a modified 21 ft. long competition ski boat solely for the purpose of gathering experimental data. The hull was made using a production mold and the modifications were limited to changes in the laminate schedule and outfitting of the boat.

“Hydrodyne’s standard construction consisted of a cored laminate schedule in which E-glass roving and cloth was used in conjunction with a balsa core. The balsa core was largely omitted in favor of a ¼ inch thick layer of chopped strand laminate, while the internal structure (longitudinal frames) remained unchanged. Additionally, no pigment was used in the protective gel coat layer which resulted in a translucent hull that aided in the visual identification of the wetted foot print from within the boat.

“The hull was outfitted with 200 through-hull manometer taps in the port side bottom. During fitting out, the arrangements and floor-boards for the port half of the hull were excluded, allowing direct access to the manometer taps and an un-obscured view for the visual identification of the spray root location... The body plan view shows that the deadrise varies from 47 degrees at the bow to 10 degrees at the transom and a lifting strake at the chine runs the entire length of the planing surface.”



Figure 32 Recreational ski boat from Hydrodyne. Translucent hull makes location of manometer taps visible in this view. Figure reproduced from Royce (2001).

A 3D CAD model of the Hydrodyne boat was built in MultiSurf, and an IGES graphical file was exported for use in the time domain simulator. The principle characteristics of the test boat are listed in Table 1. Photos of the boat and locations of the manometer pressure sensors are included as Figure 32 and Figure 33.



Figure 33 Row of manometer taps in hull of Hydrodyne ski boat. Figure reproduced from Royce (2001).

### Geometric Model

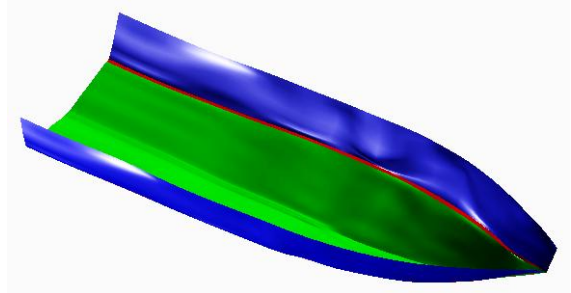
Figure 34 shows a 3D CAD model created in MultiSurf. In this figure the keel flat can be seen in the green hull bottom. The red surface is the chine flat. The MultiSurf CAD model was modified to meet the needs of the simulator, and then was exported as an IGES graphics file. The IGES file was read into the simulator and the results are illustrated by Figure 35 and Figure 36.

Table 1 Principal characteristics of Hydrodyne test boat.

LOA	20.5 ft.	Displacement	2780 lbs.
LWL	18.0 ft.	Chine Beam	5.7 ft.
LCG	6.5 ft.	Shaft Angle	15.8 degrees
VCG	1.4 ft.	Shaft Depth	1.0 ft.

### Test Program, Quasi-Static Results

To compare the results of the simulator-based pressure calculation with measured data, the Hydrodyne model was simulated at a constant speed of 20 mph in fresh water with a fixed trim angle of 3.07 degrees. The model was loaded to a weight of 2,780 lbs. to match the Royce measurements. The model was allowed to be free in heave. The simulator predicted a slightly smaller draft than was reported by Royce, but this comparison is difficult because it was unclear exactly how the draft was measured on the real boat.



• Figure 34 MultiSurf rendering of Hydrodyne recreational boat

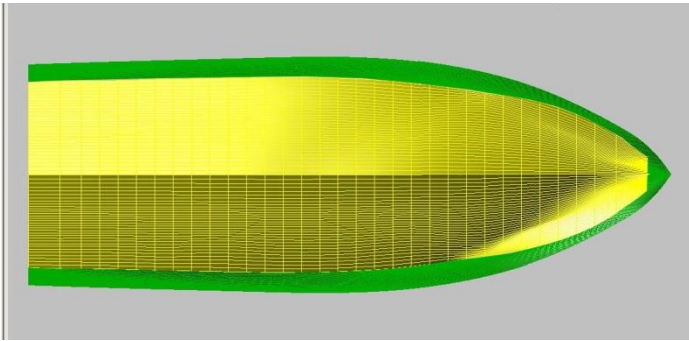


Figure 35 Rendering in plan view of model of Hydrodyne ski boat. Outer, darker section represents the actual hull. Inner, lighter section is the subset of the hull modeled in the simulator.

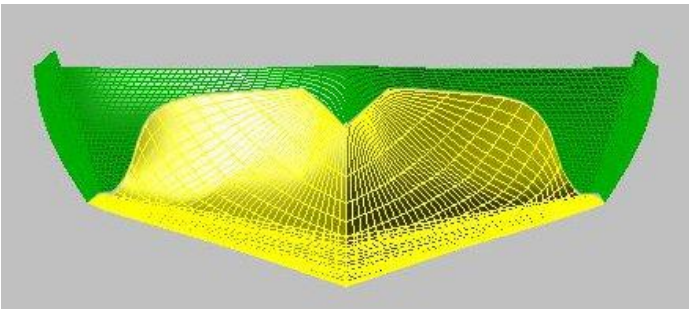


Figure 36 Rendering in bodyplan view of model of Hydrodyne ski boat. The inner, lighter section is the simulator model showing the section of bow flare included in the model.

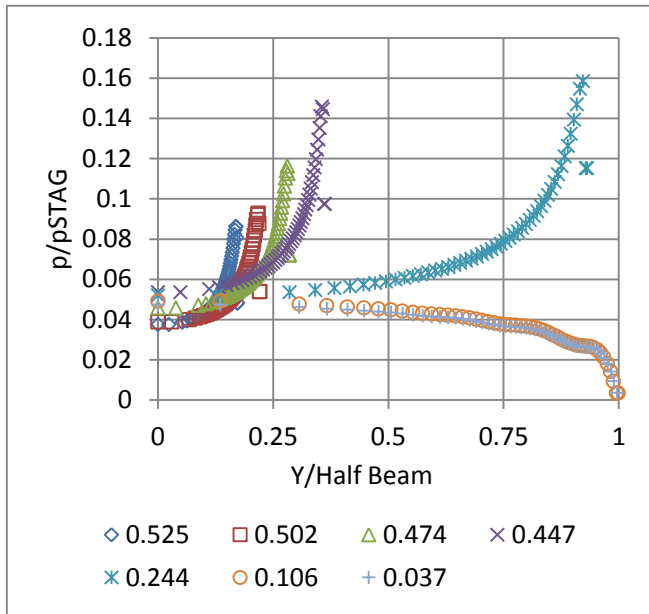


Figure 37 Transverse pressure distributions from simulation, scaled by wetted half beams and by the stagnation pressure. X coordinates of each distribution are scaled by LOA.

In Figure 37 through Figure 41 transverse coordinates Y are scaled by the individual sectional wetted beam, and pressure values are normalized by the stagnation pressure  $\frac{1}{2}\rho V^2$ . Since

results from the simulator and the actual boat varied, individual scale factors varied slightly as well. The results indicate rather good correlation between predicted and measured pressures. Figure 37 illustrates some transverse pressure distributions from the simulator analysis. Notice the pressure peaks towards the outer edge of the distributions in the chines-dry region and the tapering of distributions in the chines-wet region.

Figure 38 through Figure 41 compare the pressure distributions predicted by the time-domain simulator and measurements taken by Royce using the manometer bank in the Hydrodyne boat. In each case the longitudinal coordinate of the pressure distributions is labeled as  $X' = X / LOA$  of the boat. Because the simulator predicted a slightly different draft than was measured, slightly different calculated and measured X' locations are used in these charts.

There is tremendous variation in the measured data, but some observations can be made from these figures.

- Overall, the shape of the calculated and measured pressure distributions is similar.
- Measured data indicates more of a longitudinal drop in the chines-wet region than is predicted by the simulator.
- Due to the difference in draft predictions the mean wetted length is slightly different between the simulated and measured boats.
- The chine flat and the keel flat were not modeled as severely as they are represented in the actual boat, so there may be differences in pressure distributions in the experimental data due to rapid change in transverse deadrise.

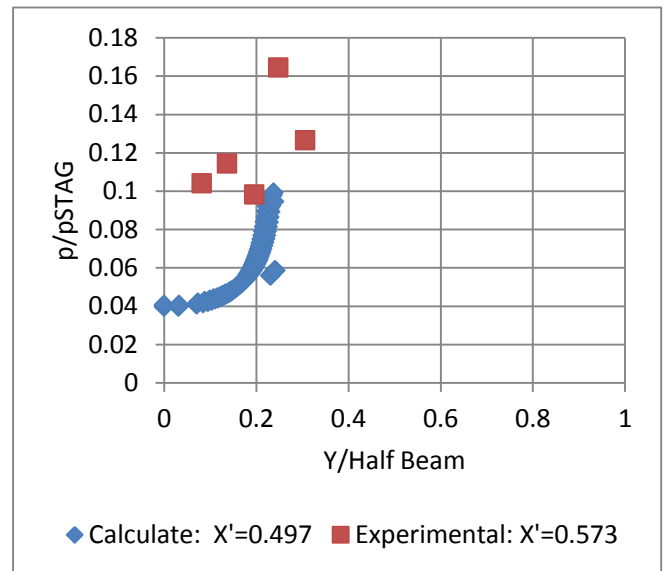


Figure 38 Measured and calculated transverse pressure distribution in forward chines-wet region. Scaled by wetted half beams and by the stagnation pressure.

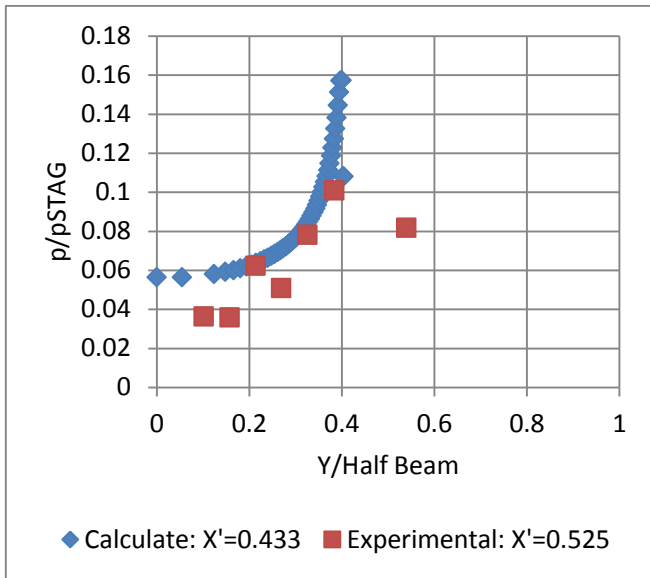


Figure 39 Measured and calculated transverse pressure distribution in chines-wet region. Scaled by wetted half beams and by the stagnation pressure.

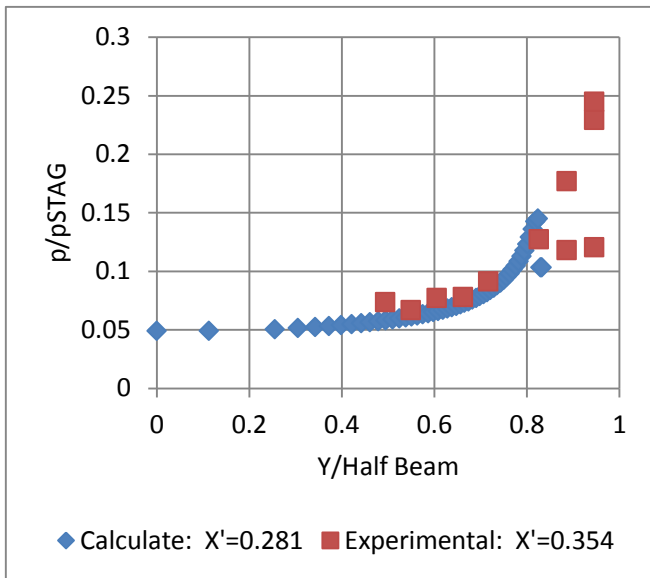


Figure 40 Measured and calculated transverse pressure distribution aftward in the chines-wet region. Scaled by wetted half beams and by the stagnation pressure.

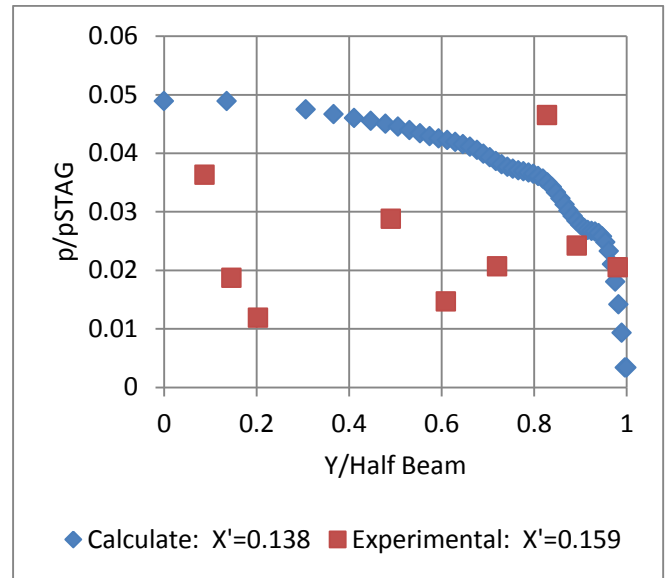


Figure 41 Measured and calculated transverse pressure distribution in chines-dry region. Scaled by wetted half beams and by the stagnation pressure.

### CONCLUSIONS

A method has been demonstrated for predicting the motions of a planing boat and for calculating the hull pressure distributions associated with the motions. The pressure distributions can be incorporated into a finite element program and used to predict the strain in the hull materials.

Future enhancements to the algorithms described here include better modeling of transverse flow separation, especially in hulls with significant spray rails and multiple chines. The existing implementation is limited to gradual changes in transverse deadrise due to the necessity for smooth geometric derivatives. Opportunities for additional research include the effects of irregular seas and of oblique headings relative to the waves. The finite element analyses were very rapid and offer the intriguing opportunity to more closely couple the simulator and the finite element solver for tasks such as optimization and long-term fatigue analyses.

### ACKNOWLEDGEMENTS

This work was supported in part by Ship Structure Committee Project SR-1470.

### REFERENCES

- ABS (American Bureau of Shipping). *RULES FOR BUILDING AND CLASSING HIGH-SPEED NAVAL CRAFT*, American Bureau of Shipping, Houston, TX, 2013 (downloaded from "http://www.eagle.org" 12-Feb-2014).
- Akers, Richard H. "Dynamic Analysis of Planing Hulls in the Vertical Plane," Presented to Society of Naval Architects and Marine Engineers, New England Section, April 29, 1999a.

- Akers, Richard H., Hoeckley, Stephen A., Peterson, Ronald S., and Troesch, Armin W. "Predicted vs. Measured Vertical-Plane Dynamics of a Planing Boat," *5th Int. Conf. on Fast Sea Transportation FAST*, 1999b.
- Brogli, R., A. Iafrati, A. "Hydrodynamics of Planing Hulls in Asymmetric Conditions," *28th Symposium on Naval Hydrodynamics*, Pasadena, California, 12-17 September 2010.
- Ensign, W., Hodgdon, J. A., Prusaczyk, W. K., Shapiro, D., and Lipton, M. "A Survey of Self-Reported Injuries among Special Boat Operators," Report No. 00-48, Naval Health Research Center, San Diego, CA, Nov. 2000.
- Fridsma, Gerard. *A Systematic study of the Rough Water Performance of Planing Boats (Irregular Waves -- Part II)*. Report 11495, Davidson Laboratory, Stevens Institute of Technology, Hoboken, New Jersey, 1971.
- Garme K. *Time-domain model for high-speed vessels in head seas [Thesis]*. KTH, Department of Vehicle Engineering; 2000.
- Heller, S. R. Jr., and Jasper, N. H. "On the Structural Design of Planing Craft," *Quarterly Transactions of the Royal Institution of Naval Architects*, July, 1960.
- IGES, *Initial Graphics Exchange Specification, IGES 5.3*, U.S. Product Data Association, N. Charleston, SC, 1997.
- IGES/PDES Organization (September 23, 1996), Initial Graphics Exchange Specification: IGES 5.3, N. Charleston, SC: U.S. Product Data Association, "Formerly an ANSI Standard September 23, 1996 – September 2006".
- Kapryan, W. J., Boyd, Jr., G. M. *Hydrodynamic Pressure Distributions Obtained During a Planing Investigation of Five Related Prismatic Surfaces*, National Advisory Committee For Aeronautics, Technical Note 3477, Langley Aeronautical Laboratory, Langley Field, VA, September 1955.
- Korvin-Kroukovsky, B. V., and Chabrow, Faye R.: The Discontinuous Fluid Flow past an Immersed Wedge. Preprint No. 169, S.M.F. Fund Paper, Inst. Aero. Sci. (Rep. No. 334, Project No. NR 062-012, ONR, Exp. Towing Tank, Stevens Inst. Tech.), Oct. 1948.
- Martin, M., Theoretical Predictions of Motions of High-Speed Planing Boats in Waves. David W. Taylor Naval Ship Research and Development Center, DTNSRDC#76/0069, 1976.
- Pierson, John D.: On the Pressure Distribution for a Wedge Penetrating a Fluid Surface. Preprint No. 167, S.M.F. Fund Paper, Inst. Aero. Sci. (Rep. No. 336, Project No. NR 062-012, ONR, Exp. Towing Tank, Stevens Inst. Tech.), June 1948.
- Pierson, John D., and Leshnover, Samuel: A Study of the Flow, Pressures, and Loads Pertaining to Prismatic Vee-Planing Surfaces. S.M.F. Fund Paper No. FF-2, Inst. Aero. Sci. (Rep. No. 382, Project No. NR 062-012, ONR Exp. Towing Tank, Stevens Inst. Tech.), May 1950.
- Rosén, A. "Loads and Responses for Planing Craft in Waves", PhD Thesis, TRITA-AVE 2004:47, ISBN 91-7283-936-8, Division of Naval Systems, KTH, Stockholm, Sweden, 2004.
- Royce, Richard. Thesis: "2-D Impact Theory Extended to Planing Craft with Experimental Comparisons," University of Michigan, August 2001.
- Savitsky, D. "Hydrodynamic Design of Planing Hulls," *Marine Technology*, 1, 1, pp. 71-95, 1964.
- Shuford, Charles L., Jr., "A Theoretical and Experimental Study of Planing Surfaces Including Effects of Cross Section and Plan Form," NACA Report-1355; 1958.
- Smiley, Robert F.: A Semiempirical Procedure for Computing the Water Pressure Distribution on Flat and V-Bottom Prismatic Surfaces During Impact Or Planing. NACA TN 2583, Langley Aeronautical Laboratory, Washington, DC, December 1951.
- Spencer, John. "Structural Design of Crewboats," *Marine Technology*, 12, 3, pp. 267-274, 1975.
- Stone, Kevin F., P.E. *Comparative Structural Requirements for High Speed Craft*, Report Number SSC-439, Ship Structure Committee, Washington, DC, February 2005.
- Tveitnes, T., Fairlie-Clarke, A.C. and Varyani, K. "An experimental investigation into the constant velocity water entry of wedge-shaped sections," *Ocean Engineering*, 35:14-15, 1463-1478, 2008.
- USCG. Structural Plan Review Guidelines for Aluminum Small Passenger Vessel, Navigation and Vessel Inspection Circular No. 11-80. U. S. Coast Guard, Washington, D.C., 1980.
- Von Karman, T., *The Impact on Seaplane Floats during Landing*, National Advisory Committee for Aeronautics (NACA), TN-321, Washington, DC, 1929.
- Vorus, William S., "A Flat Cylinder Theory for Vessel Impact and Steady Planing Resistance". *Journal of Ship Research*, Vol. 40(2), pp 89-106, 1996.
- Wagner H., Über Stoss-und Gleitvorgänge an der Oberfläche von Flüssigkeiten. *Z. angew. Math. Mech.*;12(4):193–215, 1932.
- Wittig, Klaus; *CalculiX USER'S MANUAL*, Version 2.6, July 6, 2013, [downloaded from [http://www.dhondt.de/cgx\\_2.6.1.pdf](http://www.dhondt.de/cgx_2.6.1.pdf), 26-Jan-2014].
- Zarnick, Ernest E. "A Nonlinear Mathematical Model of Motions of a Planing Boat in Regular Waves". David W. Taylor Naval Ship R & D Center, DTNSRDC-78/032, 1978.

## APPENDIX 1: PLANING HULL TIME-DOMAIN SIMULATOR

### Overview of Simulator System

Zarnick (1978) described a low-aspect ratio strip theory that can be used to predict the vertical-plane motions of planing craft.

The theory described in Zarnick's paper is the basis for the simulator program used in this project.

### Capabilities of Planing Boat Simulator

To support metocean data from a wide variety of courses, the simulator can synthesize regular and irregular seas according to Pierson-Moskowitz, JONSWAP, ITTC and Ochi 6-Parameter spectra. Thrust is applied through a thrust vector, typically the propeller shaft, or at the center of gravity.

Post-processing capabilities include Fourier transforms and spectral density functions of motions, statistical summaries of motions, motion-sickness dosage values, and Static Effective Dosage (SED) per ISO 2651.

### Calculating Forces and Moments; Simulating Motion

At each time step the time-domain simulator calculates sectional pressure contributions from the following sources:

- Impacting wedge (low aspect ratio strip theory)
- 2D ideal flow to model buttock flow. Results from panel code are adjusted for extremely low aspect ratios.
- Crossflow drag for sections in the chines-wet region
- Viscous drag with a drag coefficient based on the mean wetted length
- Hydrostatic buoyancy

The results are weighted and added together on a section-by-section basis to calculate an array sectional force vectors.

At each time step, the simulator:

1. Calculates the force vector and moment vector contributed by each station
2. Calculates the added mass contributed by each station
3. Integrates the station force and moment vectors over the entire hull to find the total force vector and moment vector
4. Integrates the added mass over the entire hull to find the total added mass and added pitch inertia
5. Solves the equations of motion to find instantaneous angular and radial accelerations:

$$|A| = (|M| + |\text{Added M}|)^{-1} * |\text{Total Force/Moment}|$$

6. Integrates the accelerations to find velocities and the velocities/angular rates to find positions/angles

The sectional force and moment vectors calculated in Step 1 are the basis for calculating the vector forces exported to FEA.

### Geometry Algorithms

The geometry kernel in the planing hull simulator is critical. Surfaces must be smooth and continuous, and it must be possible to compute surface coordinates at any point on the surface. Recognizing that the IGES 5.3 specification (IGES, 1997; IGES/PDES, 2006) describes most curve and surface types used in CAD tools, the IGES specification was used as the basis for the geometric kernel. Most of the geometric entities in the specification are supported in the geometry kernel including points, curves and surfaces. The CAD human interface supports provisions for creating and editing points, lines, parametric curves and ruled surfaces. Boat hulls may be defined using BSpline surfaces, NURBS surfaces, surfaces of rotation,

and other IGES entities, but these must be created outside of the simulator environment and imported into the simulator.

A mesh consisting of a list of hydrodynamic sections and hydrodynamic buttock lines is derived from the geometric entities that define the hull. These lines are created by:

- Finding the intersection points of station and buttock planes with all of the hull entities,
- Adjusting the intersection points so that the order of points is monotonic and the deadrise is between 0 and 90 degrees.

The points in the sorted point set become the vertices for piecewise-linear stations and buttock lines. If the user specifies reasonable resolution values then the accuracy of the results rivals the accuracy of direct calculations of each vertex.

The heart of the planing hull simulator system is a geometry program module that manages geometric entities, updates any dependencies when one of the entities is modified, and allows geometric operations such as calculating distances, intersections and areas based on the entities.

Each surface in the simulator is defined by a set of polynomials based on  $u$  and  $v$ :

$$X = fX(u, v)$$

$$Y = fY(u, v)$$

$$Z = fZ(u, v)$$

When the simulator updates the surface internally, it steps  $u$  and  $v$ , calculating  $(X, Y, Z)$  vertices at each step. Surfaces thus are defined by triangles connecting the nearest vertices. This is a simple form of tessellation, a common practice in CAD software. In Figure 42 dark green, straight lines (roughly vertical) represent constant  $U$ - and  $V$ -parameter lines on a parametric (e.g. BSpline) surface. The surface is broken into triangles by finding an array of vertices located in the surface, and then connecting the vertices with lines. Intersection lines (stations, waterlines and buttock lines) are found by computing the intersections between the triangle edges and the cutting planes.

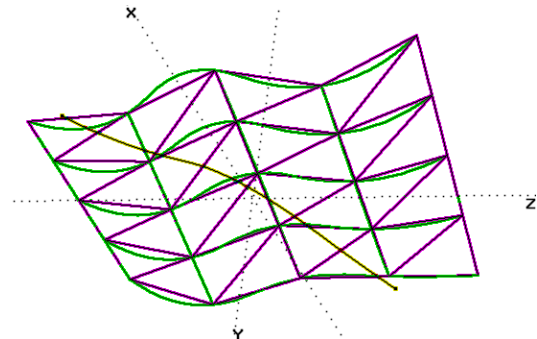


Figure 42 Tessellating a surface

### Force Algorithms in the Simulator

POWERSEA calculates five different forces acting on the hull and uses a weighted sum to calculate overall forces and moments to use in the equations of motion (refer to Figure 43):

Buoyancy

- Impacting Wedge in Chines-Dry Region
- Crossflow Drag in Chines-Wet Region

- Viscous Drag
- Dynamic lift due to Buttock Flow

**Nomenclature**

<u>Var.</u>	<u>Definition</u>
A	Acceleration vector, inertial coords.
AR	Sectional aspect ratio
b	Sectional wetted beam
$b_{HCalm}$	Half wetted beam with respect to calm water
$b_{HPileup}$	Half wetted beam with pile-up water
A	Added mass matrix (surge, heave, pitch)
$B_w$	Sectional wetted beam
$C_{D,C}$	Crossflow drag coefficient (chines-wet region)
$C_F$	Friction coefficient calculated from Mean Wetted Length using Prandtl-Schlichting line
$C'_m$	Added mass coefficient
$C_{my}$	Added mass coefficient including pileup factor
$C_{ps}$	Sectional pressure coefficient corrected for aspect ratio
$C_{ps0}$	Sectional pressure coeff. from buttock flow
$D_s$	Sectional drag force from buttock flow
$f_{CDC}$	Sectional crossflow lift (normal to baseline)
$f_D$	Sectional friction drag
$f_s$	Panel force from buttock flow at given section
$g_i$	Sectional wetted girth
I	Pitch moment of inertia of boat
$I_a$	Total added pitch inertia of boat
$k_a$	Added mass coefficient
$L_B$	Buttock length
$L_s$	Sectional lift force from buttock flow
M	Total mass of boat
$M_a$	Total added mass of boat
$m_a$	Sectional added mass
$m_i$	(Added mass theory) particle of water moving at velocity $v_i$
$m_{average}$	(Added mass theory) apparent mass of water moving with plate
$t_{pileup}$	Wetted draft of section (including pileup)
$T, T_x, T_z$	Thrust vector, x and z components (inertial)
U, V	Horiz. and vertical velocity in boat coordinates
$U_\infty$	Surge velocity for buttock flow
$v_i$	Sectional velocity in boat coordinates
$v_{plate}$	Vertical speed of plate

<u>Var.</u>	<u>Definition</u>
WF	Wetting factor that relates calm water beam to fully wetted beam
$w_x$	Horiz. component of the wave orbital velocity, inertial coords.
$\bar{x}$	State variable vector
X, Z	Horiz and vertical coords. in inertial coordinates. +X forward, +Z down
$X_{CG}, Z_{CG}$	Loc. of Center of Gravity of boat, Inertial coords.
$x_p$	Moment arm for thrust (propulsion) vector
$\beta$	Global deadrise of wedge or section (radians)
$\theta$	Boat pitch angle (radians).
$\rho$	Density of water
$\xi, \zeta$	Horiz. and vertical coords. in boat coordinate system

**Impacting Wedge (Low Aspect Ratio Strip Theory)**

Zarnick (1978) formulated a mathematical model of forces acting on a planing craft. His method assumes that wavelengths will be large with respect to the craft's length and that wave slopes will be small. Following the work of Martin (1976), Zarnick developed a mathematical formulation for the instantaneous forces on a planing craft by modeling it as a series of strips or impacting wedges. Zarnick derived the normal hydrodynamic force per unit length as:

$$f = - \left\{ \frac{D}{Dt} (m_a V) + C_{D,C} \rho b V^2 \right\} \quad (11)$$

Where  $\frac{D}{Dt} (m_a V) = m_a \dot{V} + \dot{m}_a V - \frac{\partial}{\partial \xi} (m_a V) \frac{d\xi}{dt}$  (12)

Zarnick modeled sectional added mass as an impacting wedge:

$$m_a = k_a \frac{\pi}{2} \rho b^2 \text{ and } \dot{m}_a = k_a \pi \rho b \dot{b} \quad (13)$$

where  $k_a$  is an empirical added mass coefficient.

Zarnick used the value  $k_a = 1.0$  from the derivation of Wagner (1932). The horizontal component  $w_x$  of the wave orbital velocity is considered small with respect to  $\dot{X}_{CG}$  so only the vertical component  $w_z$  is included. The boat relative velocities with the vertical wave component included are:

$$U = \dot{x}_{CG} \cos(\theta) - (\dot{z} - w_z) \sin(\theta) \quad (14)$$

$$V = \dot{x}_{CG} \sin(\theta) + (\dot{z} - w_z) \cos(\theta) - \dot{\theta} \xi \quad (15)$$

A summary of the forces acting on the planing craft is:

$$f_N = m_a \dot{V} + \dot{m}_a V - U \frac{\partial m_a V}{\partial \xi} + C_{D,C} \rho b V^2 \quad (16)$$

$$F_Z = - \int_L (f_N \cos(\theta) - C_{BF} \rho g a) d\xi \quad (17)$$

$$F_X = - \int_L f_N \sin(\theta) d\xi \quad (18)$$

$$F_\theta = \int_L (f_N - C_{BM} \rho g a \cos(\theta)) \xi d\xi \quad (19)$$

Hydrostatic forces and moments must be included in the analysis, but are difficult to predict. Water rise at the bow of a

planing vessel increases hydrostatic lift, flow separation at the stern decreases hydrostatic lift, and both cause an increase in pitching moment. These effects are speed dependent, and there is no single factor that can be used to correct the hydrostatics calculations for flow separation. In his work on rectangular planing surfaces, Shuford (1958) suggested that hydrostatic buoyancy should be halved in a dynamic simulation in order to achieve the correct total lift force, and Zarnick used an additional factor of one-half for the hydrostatic moment resulted in an accurate trim angle. In Equation 17 and Equation 19 coefficients  $C_{BF}$  and  $C_{BM}$  correct the vertical force and pitching moment. Zarnick set these coefficients to 0.5 based upon the recommendation of Shuford.

The time derivatives and partial derivatives of the boat-coordinate velocities are:

$$\dot{V} = \dot{x}_{CG} \sin(\theta) - \dot{\theta} \xi + \dot{z}_{CG} \cos(\theta) - \dot{w}_Z \cos(\theta) + \dot{\theta} (\dot{x}_{CG} \cos(\theta) - \dot{z}_{CG} \sin(\theta)) + w_Z \dot{\theta} \sin(\theta) \quad (20)$$

$$\frac{\partial V}{\partial \xi} = -\dot{\theta} - \frac{\partial w_Z}{\partial \xi} \cos(\theta) \quad (21)$$

$$\frac{\partial U}{\partial \xi} = \frac{\partial w_Z}{\partial \xi} \sin(\theta) \quad (22)$$

The vertical component of the wave orbital velocity can be described by:

$$\frac{dw_Z}{dt} = \dot{w}_Z - U \frac{\partial w_Z}{\partial \xi} \quad (23)$$

$$\text{So } \dot{w}_Z = \frac{dw_Z}{dt} + U \frac{\partial w_Z}{\partial \xi} \quad (24)$$

Making these substitutions and simplifying yields:

$$\begin{aligned} F_N = & - \int_L m_a \cos(\theta) \dot{z}_{CG} d\xi - \int_L m_a \sin(\theta) \dot{x}_{CG} d\xi \\ & + \int_L Q_a \dot{\theta} d\xi + \int_L m_a \dot{\theta} (\dot{z}_{CG} \sin(\theta) - \dot{x}_{CG} \cos(\theta)) d\xi \\ & + \int_L m_a \frac{dw_Z}{dt} \cos(\theta) d\xi - \int_L m_a w_Z \dot{\theta} \sin(\theta) d\xi \\ & - \int_L m_a V \frac{\partial w_Z}{\partial \xi} \sin(\theta) d\xi + \int_L m_a U \frac{\partial w_Z}{\partial \xi} \cos(\theta) d\xi \\ & + \int_L UV \frac{\partial m_a}{\partial \xi} d\xi - \int_L m_a U \dot{\theta} d\xi \\ & - \int_L m_a U \frac{\partial w_Z}{\partial \xi} \cos(\theta) d\xi + \int_L m_a V \frac{\partial w_Z}{\partial \xi} \sin(\theta) d\xi \\ & - \int_L V \dot{m}_a d\xi - \rho \int_L C_{D,C} b V^2 d\xi \end{aligned} \quad (25)$$

Combining terms yields:

$$\begin{aligned} F_N = & - \int_L m_a \cos(\theta) \dot{z}_{CG} d\xi - \int_L m_a \sin(\theta) \dot{x}_{CG} d\xi \\ & + \int_L Q_a \dot{\theta} d\xi + \int_L m_a \dot{\theta} (\dot{z}_{CG} \sin(\theta) - \dot{x}_{CG} \cos(\theta)) d\xi \\ & + \int_L m_a \frac{dw_Z}{dt} \cos(\theta) d\xi - \int_L m_a w_Z \dot{\theta} \sin(\theta) d\xi \\ & + \int_L UV \frac{\partial m_a}{\partial \xi} d\xi - \int_L m_a U \dot{\theta} d\xi \end{aligned}$$

$$- \int_L V \dot{m}_a d\xi - \rho \int_L C_{D,C} b V^2 d\xi \quad (26)$$

The acceleration terms  $\ddot{x}_{CG}$ ,  $\ddot{z}_{CG}$  and  $\ddot{\theta}$  are estimated using a numerical technique based on a running interpolation-polynomial estimate of state variable derivatives. The term  $\frac{\partial m_a}{\partial \xi}$  is calculated using numerical derivatives.

Combining all terms into a single integral over the boat length  $L$ , a sectional hydrodynamic normal force can be calculated as:

$$\begin{aligned} f_N = & -m_a \cos(\theta) \dot{z}_{CG} - m_a \sin(\theta) \dot{x}_{CG} \\ & + m_a \ddot{\theta} + m_a \dot{\theta} (\dot{z}_{CG} \sin(\theta) - \dot{x}_{CG} \cos(\theta)) \\ & + m_a \frac{dw_Z}{dt} \cos(\theta) - m_a w_Z \dot{\theta} \sin(\theta) \\ & + UV \frac{\partial m_a}{\partial \xi} - m_a U \dot{\theta} \\ & - V \dot{m}_a - C_{D,C} \rho b V^2 \end{aligned} \quad (27)$$

The total normal force is  $F_N = \int_L f_N d\xi$ . A similar analysis is used to obtain an estimate of the instantaneous pitching moment.

#### Wetting Factor and Added Mass

POWERSEA combines semi-empirical algorithms to predict instantaneous forces and motions on a planing craft operating in irregular waves. By adding the force components and multiplying by the inverse of the sum of the inertial masses and the instantaneous added mass of the water, it is possible to predict the accelerations of the boat in three degrees of freedom. Integrating the accelerations produces the velocities (rates), and integrating again produces the time-dependent positions (angles).

The term ‘‘added mass’’ describes a fictional amount of fluid that moves synchronously with the movements of another object submerged in the fluid. In reality there is not a single volume of water that moves at the same rate as the object, adding to the apparent mass of the object, but rather a large mass of fluid particles that are set in motion at various speeds by the moving object. The aggregate hydrodynamic force applied to the object by these particles moving in their own trajectories can be expressed in terms of a fixed (smaller) mass that is moving exactly as the object moves. A two-dimensional flat plate oscillating at very high frequencies in an ideal fluid will cause a momentum change in the fluid such that the total derivative of the momentum change will appear to be caused by a constant mass moving in the same way as the plate. This effective mass will appear to equal that of a cylinder centered on the plate:

$$\begin{aligned} \frac{d(\text{momentum})}{dt} &= \sum_{\text{Sections}} \frac{d(m_i v)}{dt} \\ &= \sum_{\text{Sections}} m_{\text{average}} * \frac{d(v_{\text{plate}})}{dt} \end{aligned} \quad (28)$$

The amount of fluid that moves with a plate with non-zero thickness can be shown to be less than that associated with a

thin flat plate. POWERSEA calculates the added mass of a boat planing on the surface, so only one-half of the cylinder is used as the basis for the added mass. The sectional added mass is the mass of a semicircle centered below the station:

$$Area = \frac{\pi}{2} \rho b_{HCalm}^2 \quad (29)$$

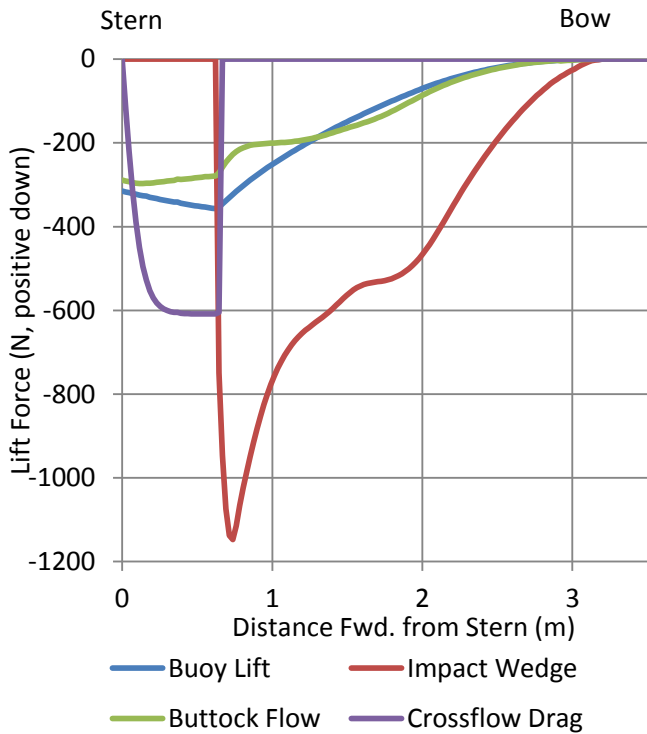


Figure 43 Force components in planing hull simulator

The sectional added mass is the effective amount of water moving under the impacting wedge as it penetrates the surface. An added mass coefficient  $c_{my}$  is defined as a function of deadrise.

$$m_A = C_{my} * \pi/2 * \rho * b_{HCalm}^2 \quad (30)$$

$$C_{my} = K_a / W F^2$$

$$K_a = f(\beta)$$

From impacting wedge theory the forces on the Chines-Dry region of a planing craft arise from the change in momentum of the added mass of water associated with each section. This force is described mathematically as:

$$F = \frac{D(m*v)}{Dt} \quad (31)$$

Where “D/Dt” is the substantial derivative operator acting on the momentum ( $m * v$ ):

$$\frac{Df}{Dt} \equiv \frac{\partial f}{\partial t} + \vec{v} \odot \nabla f$$

This represents the force from successively deeper sections of the boat as it passes in front of a stationary observer. The

velocity  $v$  is the vertical component of the velocity impacting on the hull (in boat-coordinates), and the mass  $m$  is the added mass of the water moving with the hull. In quasi-static planing operation (steady-state, no waves, constant heave, pitch and surge velocity), the added mass increases as the hull sections plunge successively deeper in the water, while the impacting rate of successive sections is constant.

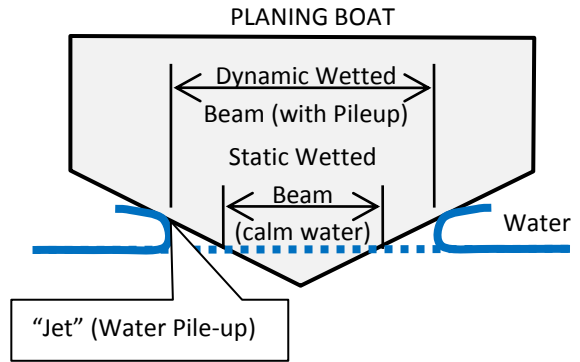
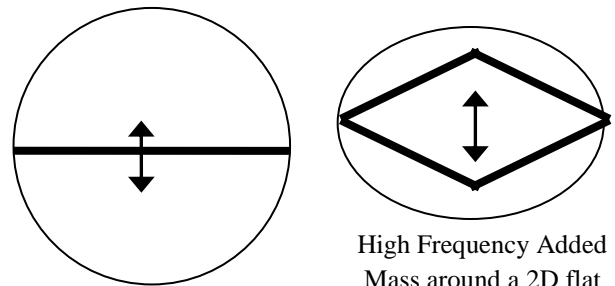


Figure 44 Water pile-up and transverse jets cause wetted-beam to be larger than static beam.



High Frequency Added Mass around a 2D flat plate.

High Frequency Added Mass around a 2D flat plate with deadrise.

$$m_A = \rho \pi r^2$$

$$m_A = k_a * \rho \pi r^2$$

Figure 45 As a V-bottomed planing boat passes through the water, the water piles up transversely along the hull bottom

Von Karman developed an expression for the added mass under an impacting wedge (Von Karman, 1929) based on a semicircle under the projected calm-water beam of the wedge:

$$y = \text{submergence} = \frac{\text{beam}}{\tan \beta} \quad (32)$$

$$m_a = \frac{\pi}{2} \rho \left( \frac{\text{beam}}{\tan \beta} \right)^2 = \frac{\pi}{2} \frac{\rho y^2}{\tan^2 \beta} \quad (33)$$

Wagner modified von Karman’s solution by accounting for the effect of water pile-up on the edges of the wedge as it enters the water (Wagner, 1932):

$$b_{HCalm} = \text{Calm water half beam} = \frac{y}{\tan \beta} \quad (34)$$

$$b_{HPileup} = \frac{\pi}{2} b_{HCalm} \quad (35)$$

$$m_a = \frac{\pi}{2} \rho b_{HPileup}^2 = \frac{\pi}{2} \rho \left( \frac{\pi}{2} b_{HCalm} \right)^2 \quad (36)$$

In the formulation in Equation 36 the wetting factor is  $\frac{\pi}{2}$ .  $C'_m$  is a non-dimensional factor defined as the ratio of the theoretical added mass to von Karman's added mass (which is the semicircle below the calm water projection). The added mass coefficient for Wagner's formulation is:

$$C'_m = \left( \frac{\pi}{2} \right)^2 \quad (37)$$

A wetting factor (WF) is defined as the ratio of the dynamic wetted beam and the static (zero speed) wetted beam. The wetting factor is a non-linear function of the global deadrise  $\beta$ . Zarnick assumed that the water pileup factor was  $\pi/2$  so that the depth of penetration is:

$$d_e = \frac{\pi}{2} * draft = WF * draft \quad (38)$$

Tveitnes, et al. (2008) investigated the water rise from impacting wedges and compared fomulations from Band, Vorus and Zhao. Vorus developed a robust model for the wetting factor (Vorus, 1996) and his work was used as the basis for the wetting factor model in POWERSEA. Data calculated using Vorus's method was fit to a quadratic regression model of the form:

$$WF(\beta) = d_1 + \beta (d_2 + \beta d_3) \quad (39)$$

Where  $d_1$ ,  $d_2$ , and  $d_3$  are regression coefficients. The coefficients for this model are listed in Table 2. Data points calculated using Vorus's model and a curve calculated from the regression model used in the simulator are included in Figure 46.

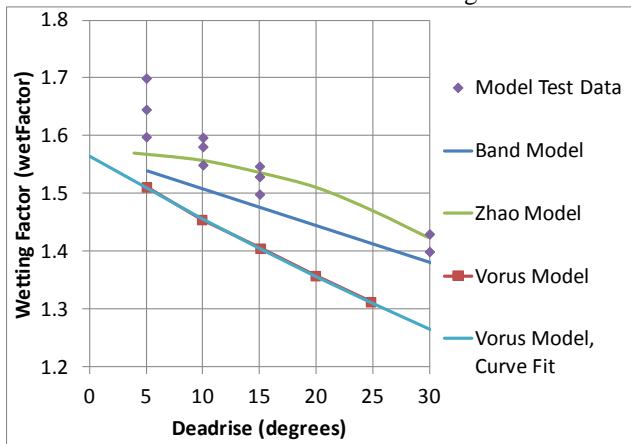


Figure 46 Wetting Factor (Dynamic Wetted Beam vs Static Wetted Beam)

Table 2 Regression coefficients for wetting factor model

Coefficient	Value
d1	1.56528
d2	-0.64721
d3	0.14048

Using this empirical formula, the wetted beam of a wedge with a constant vertical velocity is

$$b_{HPileup} = WF(\beta) * b_{HCalm} = WF(\beta) \frac{draft}{\tan \beta} \quad (40)$$

The literature describes two different added mass factors,  $C'_m$  and  $C_{my}$ .  $C_{my}$  is a vertical added mass factor which is defined as  $C_{my} = C'_m * WF^2$ . An empirical added mass coefficient  $K_a$  is defined to fit measured data and  $C_{my}$  is redefined as:

$$C_{my} = (K_a * WF) * WF = K_a WF^2 \quad (41)$$

Zarnick (1978) modeled the added mass of a section as a semicircle whose width is the "wetted beam" of the section. In the present formulation Zarnick's wetting factor of  $\frac{\pi}{2}$  was replaced with the empirical wetting factor WF:

$$\begin{aligned} m_a &= K_a \frac{\pi}{2} \rho b_{HPileup}^2 = K_a \frac{\pi}{2} \rho \left( \frac{\pi}{2} b_{HCalm} \right)^2 \\ &= C_{my} WF \frac{\pi}{2} \rho b_{HCalm}^2 \end{aligned} \quad (42)$$

The algorithm for modeling added mass in the simulator starts by calculating the wetted beam, which is then used along with  $C'_m$  to calculate instantaneous sectional added mass.

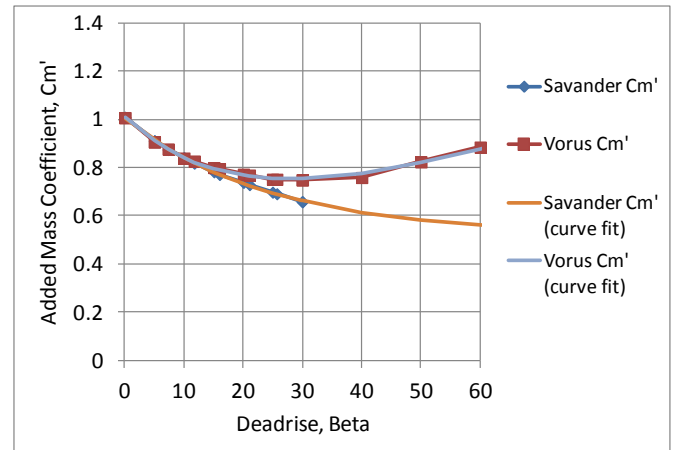


Figure 47 Added Mass coefficient versus deadrise

The relationships between several added mass formulations are shown in Figure 46. From the literature a common factor in added mass coefficient formulations is the basis function:

$$Basis Function = \left( \frac{\pi}{2\beta} - 1 \right) * 2 * \frac{\tan \beta}{\pi} \quad (43)$$

This function was used as the basis for regression models of the Savander and Vorus formulations. As can be seen in Figure 47, the numerical approximations are quite close to formulations of Vorus and Savander. The planing hull simulator models the added mass coefficient  $K_a$  with an empirical model. The derivative of the added mass coefficient with respect to deadrise  $\frac{dK_a}{d\beta}$  is a closed form expression calculated directly from the regression models of the Vorus/Savander formulations.

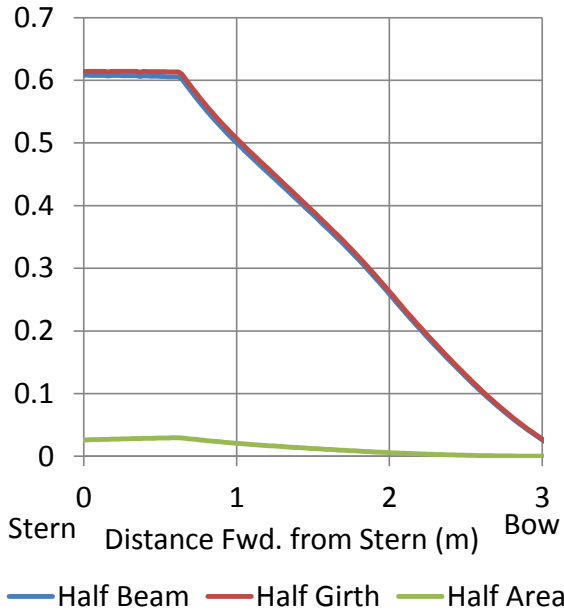


Figure 48 Simulator precalculates geometric properties at each section. Properties are based on wetted area which includes water pileup.

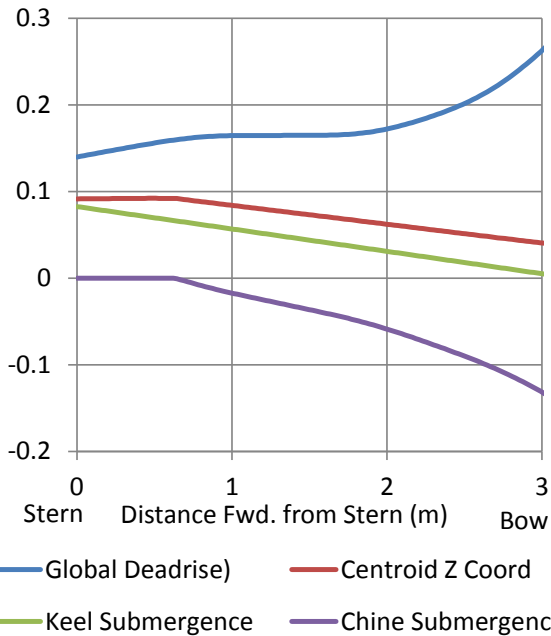


Figure 49 Precalculated geometric properties at each section For computational efficiency (Figure 48, Figure 49), the simulator precalculates the values of static wetted beam  $b_{HCalm}$  and dynamic wetted beam  $b_{HPileup}$  versus submergence (draft), and creates spline models of the relationships. During each iteration in a time-domain simulation, the simulator finds the

derivatives of  $b_H$  with respect to draft by differentiating the spline functions created for each section. To calculate the substantial derivative of the sectional momentum it is necessary to calculate the time derivative of the sectional added mass:

$$m_a = c_{my} \left( \frac{\pi}{2} \rho b_{HCalm}^2 \right) \quad (44)$$

$$C_{my} = K_a W F^2 \quad (45)$$

$$\frac{dm_a}{dt} = \frac{\pi}{2} \rho * \left( \frac{dc_{my}}{d\beta} \frac{d\beta}{dt} b_{HPileup}^2 + 2c_{my} b_{HPileup} \frac{db_{HPileup}}{dt} \right) \quad (46)$$

$$\frac{dC_{my}}{d\beta} = \frac{\partial K_a}{\partial \beta} W F^2 + 2 K_a W F \frac{dWF}{d\beta} \quad (47)$$

A station is described by a piecewise linear curve connecting vertices that are found during the meshing operation. The global deadrise of a station is defined as the arctangent of the slope of the submerged portion of the station,  $\frac{\partial z}{\partial y} = \frac{b_{HPileup}}{t_{Pileup}}$ , where  $t_{Pileup}$  is the draft of the section including the piled up transverse jet. The time-derivative of deadrise at a station is calculated as:

$$\frac{d\beta}{dt} = \frac{d\beta}{dt_{Pileup}} * \frac{dt_{Pileup}}{dt} \quad (48)$$

$$\frac{dC_{my}}{d\beta} = \frac{dK_a}{d\beta} W F^2 + K_a W F \frac{dWF}{d\beta} \quad (49)$$

$$\begin{aligned} \frac{d\beta}{dt_{Pileup}} &= \frac{d\left(\tan^{-1} \frac{b_{HPileup}}{t_{Pileup}}\right)}{dt_{Pileup}} \\ &= \frac{1}{1 + \left(\frac{b_{HPileup}}{t_{Pileup}}\right)^2} * \frac{b_{HPileup}}{t_{Pileup}^2} \end{aligned} \quad (50)$$

$$\frac{db_{HPileup}}{dt} = \frac{db_{HPileup}}{d(draft)} * \frac{d(draft)}{dt} \quad (51)$$

The terms  $\frac{dWF}{d\beta}$ ,  $\frac{dK_a}{d\beta}$  are calculated from the empirical models and  $\frac{d(draft)}{dt}$  is estimated at every time step in the simulation.

**Buoyancy**

The planing hull simulator is intended to simulate high speed craft so the majority of the lift force arises from hydrodynamic mechanisms. Hydrostatic forces cannot be ignored, however, especially at lower planing speeds. In reality the hydrostatics and hydrodynamic forces cannot be separated, but for planing boats it is possible to make some simplifying assumptions about the hydrostatic forces and treat them separately from the hydrodynamic ones.

For most planing boats the water will separate off the bottom edge of the transom, so the wetted surface is not bow-stern symmetric. This effect is considered to be part of the impacting wedge formulation, so no hydrostatic “drag” is included in the simulator force formulation.

As illustrated in Figure 50, this choice results in a lower hydrostatic bow-down moment than would be obtained by using the calm water surface as the reference plane.

Engineers calculate hydrostatic pressure by applying the Bernoulli Equation along a streamline starting at the free surface and ending at the point of interest. In the case of a planing craft, different results are obtained if the calm water surface is used as the starting point (Figure 50, A) than if the wetted surface at the boat hull is used as the starting point (Figure 50, B).

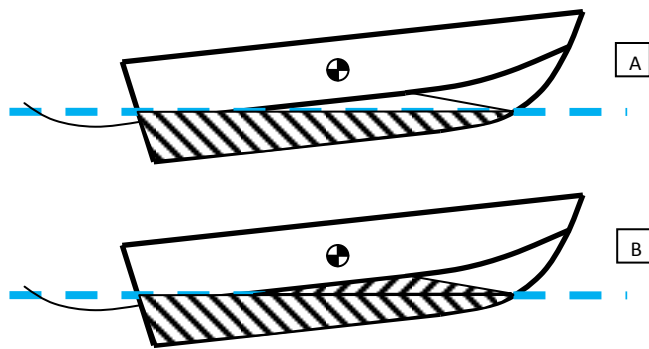


Figure 50 Calculating Displacement using calm waterline (top, A) or dynamic waterline (bottom, B). Buoyancy creates a larger bow-up moment in B than in A.

By comparing simulation results for quasi-static (constant speed) operation, it was found that more accurate results are obtained using the pile-up wetted surface on the boat hull as the zero-pressure reference height for hydrostatic pressure calculations.

The hydrostatic forces on the planing boat are not fore-aft symmetric as the transom is dry when the boat is on plane. This factor should be taken into account to calculate surge resistance accurately.

**Viscous Drag**

Special attention is paid to the friction force  $F_D$ . At each time step the mean wetted length, the Reynolds Number, and a friction coefficient can be calculated. The friction coefficient is calculated using the Prandtl-Schlichting line. For most of the hull this friction coefficient will be valid, but for highly curved sections the water flow will be significantly greater than the nominal water flow past the hull. A sectional friction force is calculated as:

$$f_D = \frac{1}{2} C_{FD} \rho v_i^2 g_i \tag{52}$$

**Crossflow Drag**

The impacting wedge algorithm does not apply to the chines-wet region because it depends on the substantial derivative of the water momentum,  $D(ma*v)/dt$ . Since the added mass  $m_a$  beneath the hull is a fixed value in the chines-wet region, a

different mechanism is required to model the dynamic force in this region. The dynamic force is modeled in this region using a drag coefficient,  $C_{DC}$ , which varies along a straight line from the start of the chines-wet-region to the transom. The sectional lift from the crossflow drag is

$$f_{CDC} = 1/2 \rho v_i^2 C_{DC} B_W \tag{53}$$

A cosine blending function is applied starting at 1/4 beam forward of the transom so that the  $C_{DC}$  coefficient drops smoothly to zero at the transom (Garne, 2000).

**Buttock Flow**

To better model dynamic lift and induced drag due to the flow of water along the bottom of planing hulls, a 2D panel code was added to the simulator. The simulator precalculates an array of drag coefficients using a panel method. This array spans multiple buttock locations, boat trim angles and buttock draft angles. During each time-step, the sectional pressure coefficient is calculated by using a quadratic interpolation between the precalculated results.

A triangular mesh is generated from the hull geometry to represent the hull surfaces. An array of 2D foils is created by intersecting the submerged portion of the mesh (using the calm water draft) along buttock planes starting from the centerplane out to 98% of the maximum beam at the chine. The resulting points are mirrored across the calm waterline and these are fitted with a foil curve (Figure 51). Additional foil curves are generated by generating buttock curves at the same buttock planes but fractions of the calm water drafts.

Using a panel code derived from a constant-strength vortex method described in Katz (1991), a matrix of pressure coefficients is calculated at the x-coordinates of a set of transverse sections along each buttock and at each draft for a range of trim angles ranging from -30 degrees to +30 degrees. These values are precalculated in a mesh operation that is performed before any time-domain simulation runs.

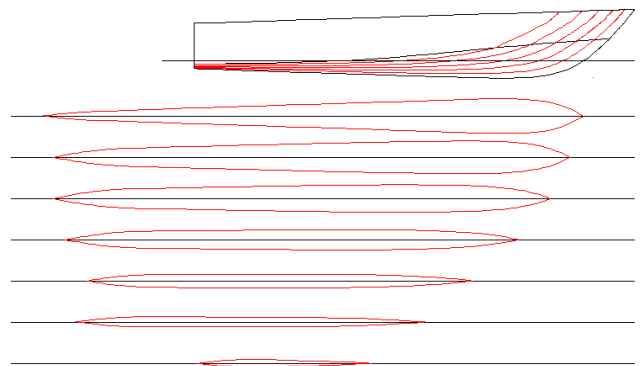


Figure 51 Planing hull with foils created from buttock curves

At each time step of an analysis, a pressure coefficient ( $C_{ps0}$ ) is calculated for each section. The pressure coefficient is obtained by finding the instantaneous half-wetted beam, draft, and trim angle of the section. Using these values the pressure coefficient

is interpolated from the matrix of coefficients previously calculated.

In Figure 52 the pressure coefficients for buttock lines are labeled by the fraction of the maximum beam (e.g. “Buttock 0.400” is located at 40% of BMax from centerplane).

A correction for low aspect ratio wings using Jones’ approximation (Jones, 1946) is applied to the pressure coefficient:

$$AR = B_w/L_B \quad (54)$$

$$C_{ps} = 0.25C_{ps0}AR * \cos(\beta) \quad (55)$$

The panel force due to pressure at any given section is calculated as:

$$f_s = \frac{\rho}{2} C_{ps} U_\infty^2 B_w \quad (56)$$

Lift ( $l_s = f_s \cos \alpha$ ) and drag ( $d_s = f_s \sin \alpha$ ) forces are derived from this panel force and the slope of the buttock curve at the given section angle of attack  $\alpha$ .

### Combining Algorithms

The planing hull simulator calculates a number of force components, but these force components are not independent from each other. The forces must be blended in a rational manner to avoid missing components or adding multiple models for the same physical effect.

Although research in this area is ongoing, the following algorithm is used to calculating linear weighting factors to combine the forces:

1. Weighting factors must be based on non-dimensional geometric characteristics, not on dynamic characteristics.
2. Weighting factors must be set and validated using model test and full-scale test data.
3. Weighting factors are polynomial functions of the principal characteristics of the model boat, but no term can have more than two characteristic factors and no factor can have an exponent outside the range of -2 to 2.

The first rule guarantees that the dynamics of the boat are a function of the force algorithms and not of the weighting factors. That is as the boat speed changes the hydrodynamics is modeled in the force equations, not in the weighting coefficients. The second rule helps to guarantee that the weighting factors result in predictions that can be extrapolated to new models for similar boats. The third rule helps to avoid numerical oscillations between the peaks and troughs of complex polynomial equations.

The results included in this report were accomplished with a fixed set of weighting coefficients that have been found to produce accurate results for a wide range of high-speed boats.

### Solving Equations of Motion

The acceleration terms can be factored out of the sectional force and moment expressions:

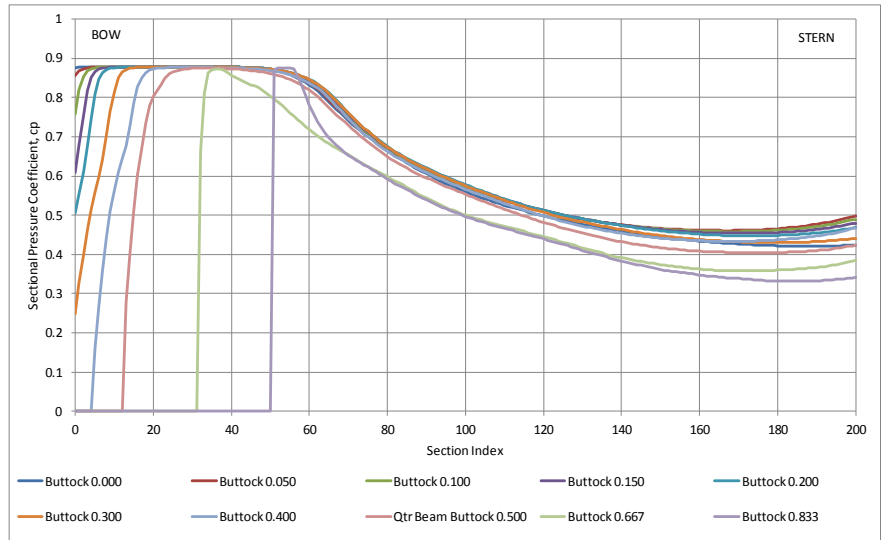


Figure 52 Pressure coefficients on buttocks from panel code (4 degree trim)

$$\begin{aligned} F'_x &= F_x - (\text{accel. terms}) \\ &= \left\{ \int_L m_a \dot{\theta} (\dot{z}_{CG} \sin(\theta) - \dot{x}_{CG} \cos(\theta)) d\xi \right. \\ &\quad + \int_L m_a \frac{dw_z}{dt} \cos(\theta) d\xi - \int_L m_a w_z \dot{\theta} \sin(\theta) d\xi \\ &\quad + \int_L \left( UV \frac{\partial m_a}{\partial \xi} \right) d\xi - \int_L m_a U \dot{\theta} d\xi - \int_L V \dot{m}_a d\xi \\ &\quad \left. - \rho \int_L C_{D,c} b V^2 d\xi \right\} \sin \theta - \int_L f_s \sin \alpha d\xi \quad (57) \end{aligned}$$

$$\begin{aligned} F'_z &= F_z - (\text{accel. terms}) \\ &= \left\{ \int_L m_a \dot{\theta} (\dot{z}_{CG} \sin(\theta) - \dot{x}_{CG} \cos(\theta)) d\xi \right. \\ &\quad + \int_L m_a \frac{dw_z}{dt} \cos(\theta) d\xi - \int_L m_a w_z \dot{\theta} \sin(\theta) d\xi \\ &\quad + \int_L \left( UV \frac{\partial m_a}{\partial \xi} \right) d\xi - \int_L m_a U \dot{\theta} d\xi \\ &\quad \left. - \int_L V \dot{m}_a d\xi - \rho \int_L C_{D,c} b V^2 d\xi \right\} \cos \theta \\ &\quad + \rho g \int_L C_{BF} A d\xi - \int_L f_s \cos \alpha d\xi \quad (58) \end{aligned}$$

$$\begin{aligned}
 F'_\theta &= F_\theta - (\text{accel. terms}) \\
 &= -(\dot{z}_{CG} \sin(\theta) - \dot{x}_{CG} \cos(\theta))\dot{\theta} \int_L m_a \xi d\xi \\
 &\quad - \cos(\theta) \int_L m_a \frac{dw_Z}{dt} \xi d\xi + \dot{\theta} \sin(\theta) \int_L m_a w_Z \xi d\xi \\
 &\quad - UV \int_L \frac{\partial m_a}{\partial \xi} \xi d\xi + U\dot{\theta} \int_L m_a \xi d\xi + V \int_L \dot{m}_a \xi d\xi \\
 &\quad + C_{D,C} \rho V^2 \int_L b \xi d\xi - \rho g \int_L C_{BF} A \xi \cos \theta d\xi \\
 &\quad - \int_L f_s \xi d\xi \tag{59}
 \end{aligned}$$

Combining the modified sectional force and moment expressions with the general equations of motion yields:

$$\begin{aligned}
 &\begin{vmatrix} M + M_a \sin^2 \theta & M_a \sin \theta \cos \theta & -Q_a \sin \theta \\ M_a \sin \theta \cos \theta & M + M_a \cos^2 \theta & -Q_a \cos \theta \\ -Q_a \sin \theta & -Q_a \cos \theta & I + I_a \end{vmatrix} * \begin{vmatrix} \ddot{x}_{CG} \\ \ddot{z}_{CG} \\ \ddot{\theta} \end{vmatrix} \\
 &= \begin{vmatrix} F'_x + T_x \\ F'_z + T_z + W \\ F'_\theta + T * X_p \end{vmatrix} \tag{60}
 \end{aligned}$$

A set of state variables  $\dot{x}_{CG}$ ,  $\dot{z}_{CG}$ ,  $\dot{\theta}_{CG}$ ,  $x_{CG}$ ,  $z_{CG}$ , and  $\theta_{CG}$ , are chosen. The matrix equation above can be written as  $|A| \dot{\vec{x}} = \vec{f}$

where  $|A|$  is the mass matrix,  $\dot{\vec{x}}$  is the derivative of the state variable vector  $(\dot{x}_{CG}, \dot{z}_{CG}, \dot{\theta}_{CG})$ , and  $\vec{f}$  is the right-hand side forcing function, which is itself a function of the state variables.

At each time step the matrix equation is solved for  $\dot{\vec{x}} = |A|^{-1} \vec{f}$ .

The resulting equations are integrated to find the new value of the state variables  $\dot{x}_{CG}$ ,  $\dot{z}_{CG}$ ,  $\dot{\theta}_{CG}$ , and the previous value of the state variables  $x_{CG}$ ,  $z_{CG}$ ,  $\theta_{CG}$  are integrated to find the new value of the state variables  $x_{CG}$ ,  $z_{CG}$ , and  $\theta_{CG}$ .